

A Dynamic Continuum Model for Traffic Assignment in an Urban City

Saksham Singh

*A dissertation submitted for the partial fulfilment
of BS-MS dual degree in Science*



Department of Mathematical Science
Indian Institute of Science Education and Research Mohali
April 2014

Certificate of Examination

This is to certify that the dissertation titled **A Dynamic Continuum Model for Traffic Assignment in an Urban City** submitted by **Saksham Singh** (Reg. No. MS09111) for the partial fulfillment of BS-MS dual degree programme of the Institute, has been examined by the thesis committee duly appointed by the Institute. The committee finds the work done by the candidate satisfactory and recommends that the report be accepted.

Prof. Kapil H. Paranjape Dr. Alok Maharana Dr. Chanchal Kumar
(Supervisor)

Dated: April 23, 2014

Declaration

The work presented in this dissertation has been carried out by me under the guidance of Dr. Chanchal Kumar at the Indian Institute of Science Education and Research, Mohali.

This work has not been submitted in part or in full for a degree, a diploma, or a fellowship to any other university or institute. Whenever contributions of others are involved, every effort is made to indicate this clearly, with due acknowledgement of collaborative research and discussions. This thesis is a bonafide record of original work done by me and all sources listed within have been detailed in the bibliography.

Saksham Singh
(Candidate)

Dated: April 23, 2014

In my capacity as the supervisor of the candidate's project work, I certify that the above statements by the candidate are true to the best of my knowledge.

Dr. Chanchal Kumar
(Supervisor)

Acknowledgment

I am delighted to see my MS thesis has eventually come through. Firstly, I would like to thank my project supervisor Dr. Arvind Kumar Gupta (Department of Mathematics, Indian Institute of Technology, Ropar) for giving me an opportunity to work under him. He was the one who first introduced me to the topic and it was really worth the effort, learning the subject. He continuously and convincingly conveyed a spirit of adventure in regard to research and an excitement in regard to learning. I am also grateful to his doctoral student Mrs. Isha Dhiman who helped me through out the year. She had very patiently worked on several algorithms of the code with me and suggested several corrections. She took pains in drafting my thesis from the very beginning. Furthermore, she also helped me with the initial problems which I faced with L^AT_EX and MATLAB. Without her guidance and persistent help this dissertation would not have been possible.

I owe special gratitude to my committee chair, Dr. Chanchal Kumar. He has been an exemplary guide in every sense, and above all, he has persisted in providing the guidance that I needed at each step.

I am also grateful to Ms. Jie Du as she was generous enough to reply my mails.

Words can not express how grateful I am to my family members, who have always been my source of inspiration.

Finally I am thankful to IISER Mohali and IIT Ropar for providing me such a pleasant environment to work and Department of Science and Technology, India for financial support by giving me INSPIRE fellowship.

Saksham Singh

List of Figures

1.1	Highway (position of cars denoted by x_i).	2
1.2	Cars entering and leaving a segment of roadway.	4
1.3	Car velocity diminishes as traffic density increases.	7
1.4	Fundamental Diagram of Road Traffic (flow-density traffic).	8
2.1	(a) A linear velocity-density curve, (b) Fundamental traffic diagram (flow-density curve).	12
2.2	Rarefaction wave under the Riemann initial condition: temporal development of speed $u(x, t)$.	15
2.3	Rarefaction waves under the Riemann initial condition: temporal development of density $k(x, t)$	16
3.1	The Modeling Domain	17
3.2	The 3D trajectory of a vehicle.	21
3.3	Solution Procedure	29
3.4	The modeling domain.	31
3.5	Density mesh at $t = 0.5h$	33
3.6	Density mesh at $t = 1h$	33
3.7	Density mesh at $t = 2h$	34
3.8	Density mesh at $t = 3h$	34
3.9	Density mesh at $t = 4h$	35
3.10	Density mesh at $t = 5h$	35
3.11	Density mesh at $t = 6h$	36
3.12	Cost potential mesh and contour at $t = 0h$	36
3.13	Cost potential mesh and contour at $t = 1h$	37
3.14	Cost potential mesh and contour at $t = 2h$	37
3.15	Cost potential mesh and contour at $t = 3h$	38
A.1	The used and unused paths.	40

A.2	Two used paths from (\tilde{x}, \tilde{y}) to the CBD.	41
B.1	The used and the unused path.	43
C.1	Two used paths.	47

Abstract

Mathematical models established on partial differential equations (PDEs) are omnipresent these days, emerging in all fields of science and engineering. Example implementation areas include fluid dynamics, quantum theory, general and special relativity, nonlinear dynamics, biology, cellular automata, cardiac modeling, finance and option pricing. Unfortunately, it is almost always impossible to acquire closed-form solutions of PDE equations, even in very simple cases. Therefore, numerical schemes for finding approximate solutions to PDE problems are of great importance.

For the opulence in both developed and developing countries, efficient traffic systems are indispensable. However, due to an overall increase of mobility and transportation during the last two decades, the capacity of the road infrastructure has been reached. Many mega cities already suffer from daily traffic collapses and their environmental consequences. More fuel consumption and air pollution is caused by impeded traffic and stop-and-go traffic. Due to such reasons, several models for freeway traffic have been proposed. Such models are used for developing traffic optimization measures like on-ramp control, variable speed limits or re-routing systems.

The continuum modeling approach to transportation models is now gaining much attention because of its advantages in dealing with macroscopic problems, initial phase planning and dense-network models. In this text we provide a comprehensive review of the of the development and application of the predictive continuum dynamic user-optimal (PDUO-C) modeling approach. We first discuss the theoretical development and then discuss some results of PDUO-C in regard of the density profiles and the cost-potential. Such profiles are useful in study of facility location, route choice, pedestrian flow, and policy and socio-economical analysis.

We examine the numerical solution to the system of partial differential equations for the conservation law governing the density, in which the flow direction is determined, and a Hamilton-Jacobi equation to compute the total travel cost using the Lax-Friedrichs scheme. The intertwined system of equations is solved by self-adaptive method of successive averages (MSA) using the least square fitting. Numerical results are demonstrated through computer simulation in MATLAB.

Contents

List of Figures	ii
Abstract	iii
1 Introduction	1
1.1 Introduction to Traffic Flow	1
1.1.1 Automobile Velocity and a Velocity Field	2
1.1.2 Traffic Density and Traffic Flow	2
1.1.3 Fundamental Law of Traffic Flow	3
1.1.4 Conservation of the Number of Cars [3]	3
1.1.5 A Velocity-Density Relationship	6
1.1.6 Traffic Flow	8
1.2 Traffic Assignment Modeling	8
2 Literature Survey	11
2.1 First Order Models	11
2.1.1 LWR Model [9]	11
2.1.2 Greenshield's Experimental Model [12]	12
2.2 Higher Order Models	12
2.2.1 H.J. Payne's Model [15]	13
2.2.2 Rui Jiang's Model [5]	13
3 A Continuum Model for Urban Cities	17
3.1 Problem Description	17
3.2 Inconsistency of the Jiang's model	19
3.2.1 Original Model (Jiang et al.) [7]	19
3.2.2 The Inconsistency [2]	19
3.3 An Improved Model (Du et al.) [2]	20

3.3.1	The derivation of the path-choice strategy in the special case that the cost is the time	20
3.3.2	Derivation of the path choice formula with a more general cost .	21
3.3.3	Relation between the Special Case and the General Case	22
3.4	The complete model and the discussion of initial boundary conditions [2]	23
3.4.1	The conservation law and its initial boundary conditions	23
3.4.2	The Hamilton-Jacobi equation and its initial boundary conditions	24
3.4.3	The Complete Model	25
3.5	Solution Algorithm [2]	25
3.5.1	Lax-Friedrichs scheme to solve the conservation law	25
3.5.2	Lax-Friedrichs scheme to solve the Hamilton-Jacobi equation . .	26
3.6	Fixed-point problem and MSA	27
3.6.1	A self-adaptive MSA [2]	29
3.7	Numerical Setting [2]	31
3.8	Numerical Results	33
3.9	Conclusions	38
A	The detailed proof of Theorem 1 [2]	39
B	The detailed proof of Theorem 2 [2]	43
C	The detailed proof of Theorem 3 [2]	47
D	Fast sweeping method to solve the Eikonal equation [2]	49

Chapter 1

Introduction

1.1 Introduction to Traffic Flow

Traffic problems have racked man long before the dawn of the automobile. Traffic flow modeling has been rapidly developed in the last two decades. In many applications, the models are merged with actual data concerned with the current traffic state and with fast computational methods. Because of this combination it has become possible to make precise and useful short term forecast about the advancement of the traffic state. Transportation problems which are governable to a scientific analysis include: where to install traffic lights or stop signs; how long the cycle of light should be; how to develop a progressive traffic light system; whether to change a two way street to one way street; whether to construct entrances, exits and overpasses; how many lanes to build for a new highway. This scientific analysis can be used to guide and notify road users, for example about substitute routes. Moreover, the forecast can be used in controlling traffic in an efficient way in order to avoid or minimize delays. The forecast in particular is useful in the case of unexpected circumstances such as an accident, uttermost weather conditions. In particular, the ultimate aim is to study traffic phenomenon in order to make decisions which may attenuate congestion, maximize traffic flow, annihilate accidents, minimize automobile exhaust pollution and other desirable ends.

In this text we do not propose to formulate all kinds of transportation problems. Instead we will focus on a problem which has recently received a mathematical formulation; how traffic flows along a unidirectional road. Instead of analyzing the behavior of individual cars, we principally study traffic situations of whole population.

In this text begin our audit of transportation problems by discussing the fundamental

traffic variables: velocity, density and flow. Conservation of cars and experimental relationship between car velocity and traffic density.

1.1.1 Automobile Velocity and a Velocity Field

Imagine a car moving along a highway. If the position of the car is designated $x_0(t)$, then its velocity is given by, $dx_0(t)/dt$ and its acceleration is $d^2x_0(t)/dt^2$. Consider a situation on highway with many cars each designated by a position $x_i(t)$, as shown in figure.

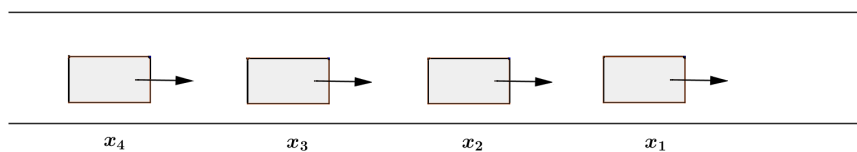


Figure 1.1: Highway (position of cars denoted by x_i).

The velocity can be measured in two ways. The most common is to measure the velocity u_i of each car, $u_i = dx_i/dt$. With N cars there are N different velocities, each depending on time, $u_i(t); i = 1, \dots, N$. In many situations the number of cars is so large that it is not possible to keep track of each car. Rather than recording the velocity of each individual car, we associate to each point in space (at each time) a unique velocity, $u(x, t)$, called a *velocity field*. This would be the velocity measured at time t by an observer fixed at position x . This velocity (at x , at time t) is the velocity of a car at that place (if car is there at that time). Expressing this statement in mathematical terms, the velocity field $u(x, t)$ at the car's position $x_i(t)$ must be the car's velocity $u_i(t)$,

$$u(x_i(t), t) = u_i(t). \quad (1.1)$$

Thus the existence of such a velocity field $u(x, t)$ implies that there exists a single velocity at each x and t . Consequently this model does not allow cars to pass each other (since at the point of passing there simultaneously must be two different velocities!).

1.1.2 Traffic Density and Traffic Flow

The number of cars per mile (per lane) is defined as the *density* of cars, ρ . In our text we assume that all vehicles are the same; the word car loosely represents any vehicle. For simplicity it is assumed that all vehicles have same length, L . If the distance

between cars is d (the distance $d + L$ is called the spacing), then the number of cars per mile(kilometers) is

$$\rho = \frac{1}{d + L}. \quad (1.2)$$

The average number of cars passing per hour (per lane) is defined as *traffic flow*, q . At different positions along the road, the flow might be different. Similarly the flow differs from time to time. Therefore the flow depends on space and time, and we write flow as a function of space and time, $q(x, t)$.

1.1.3 Fundamental Law of Traffic Flow

Consider a situation on highway where traffic is moving at a constant velocity u_0 with a constant density ρ_0 . Since the velocity is constant the distance between cars remains constant.

In τ hours each car has moved $u_0\tau$ distance, and hence the number of cars that pass the observer in τ hours is the number of cars in $u_0\tau$ distance. Since ρ_0 is the number of cars per mile and there are $u_0\tau$ miles, then $\rho_0 u_0\tau$ is the number of cars passing the observer in τ hours. Thus the number of cars per hour which we have called the traffic flow, q , is

$$q = \rho_0 u_0. \quad (1.3)$$

If the traffic variables depend on x and t , then we write,

$$q(x, t) = \rho(x, t)u(x, t). \quad (1.4)$$

1.1.4 Conservation of the Number of Cars [3]

On some interval of roadway, between $x = a$ and $x = b$, the number of cars N is the integral of the traffic density:

$$N = \int_a^b \rho(x, t)dx. \quad (1.5)$$

If there are no entrances nor exits in the road, then the number of cars between $x = a$ and $x = b$ might still change in time. Assuming that no cars are created nor destroyed in between, then the changes in the cars result from crossing at $x = a$ and $x = b$ only. If cars are flowing at a rate of $q(a, t)$ at $x = a$, but flowing at a rate of

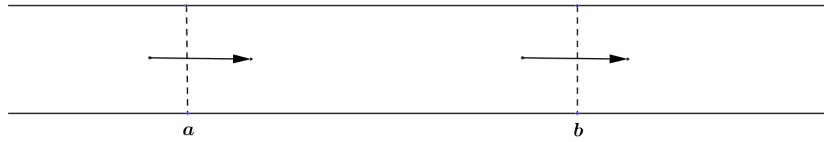


Figure 1.2: Cars entering and leaving a segment of roadway.

$q(b, t)$ at $x = b$, then the rate of change of the cars is given by

$$\frac{dN}{dt} = q(a, t) - q(b, t), \quad (1.6)$$

Since the number of cars per unit time is the flow $q(x, t)$.

Combining equations (1.4) and (1.5), yields

$$\frac{d}{dt} \int_a^b \rho(x, t) dx = q(a, t) - q(b, t). \quad (1.7)$$

This equation expresses the fact that changes in the number of cars is only due to flow across the boundary. The number of cars is conserved. Equation (1.6) is called a conservation law in integral form or, more concisely, an integral conservation law.

Consider an extremely long highway which we model by a highway of infinite length. let us assume that the flow of cars approaches zero as x approaches both $\pm\infty$,

$$\lim_{x \rightarrow \pm\infty} q(x, t) = 0,$$

From equation (1.7), it follows that

$$\frac{d}{dt} \int_{-\infty}^{\infty} \rho(x, t) dx = 0.$$

Integrating this yields

$$\int_{-\infty}^{\infty} \rho(x, t) = \text{constant},$$

which states that the total number of cars is constant for all time.

The integral conservation law, equation (1.6), is expressed as a local conservation law, valid at each position of the roadway. The endpoints of the segment of the

roadway, $x = a$ and $x = b$, are considered as additional independent variables.* Thus the full derivative with respect to time must be replaced by partial derivative,

$$\frac{\partial}{\partial t} \int_a^b \rho(x, t) dx = q(a, t) - q(b, t), \quad (1.8)$$

Consider the integral conservation of cars over a small interval of highway from $x = a$ to $x = a + \Delta a$. Thus from equation (1.7),

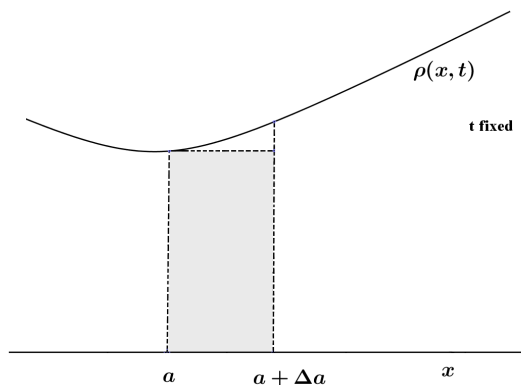
$$\frac{\partial}{\partial t} \int_a^{a+\Delta a} \rho(x, t) dx = q(a, t) - q(a + \Delta a, t).$$

Divide by $-\Delta a$ and take the limit $\Delta a \rightarrow 0$:

$$\lim_{\Delta a \rightarrow 0} \frac{\partial}{\partial t} \frac{1}{-\Delta a} \int_a^{a+\Delta a} \rho(x, t) dx = \lim_{\Delta a \rightarrow 0} \frac{q(a, t) - q(a + \Delta a, t)}{-\Delta a} \quad (1.9)$$

The right-hand side of equation (1.8) is exactly definition of the derivative of $q(a, t)$ with respect to a (properly a partial derivative should be used, since t is fixed), $(\partial/\partial a)q(a, t)$. On the left-hand of the equation (1.8) the limit is performed as follows:

(a) The integral is the area under the curve $\rho(x, t)$ between $x = a$ and $x = a + \Delta a$. Since Δa is small, the integral can be approximated by one rectangle; as shown in figure. The number of cars between a and $a + \Delta a$ can be approximated by the length of roadway Δa times the traffic density at $x = a$, $\rho(a, t)$. Thus,



$$-\frac{1}{\Delta a} \int_a^{a+\Delta a} \rho(x, t) dx \approx -\rho(a, t). \quad (1.10)$$

The error vanishes as $\Delta a \rightarrow 0$. Consequently we derive from equation (1.7) that

$$\frac{\partial}{\partial t}\rho(a, t) + \frac{\partial}{\partial a}q(a, t) = 0. \quad (1.11)$$

(b) On the other hand, introduce the function $N(\bar{x}, t)$, the number of cars on the roadway between any fixed position x_0 and the variable position \bar{x} ,

$$N(\bar{x}, t) \equiv \int_{x_0}^{\bar{x}} \rho(x, t) dx.$$

Then, the average number of cars per mile between a and $a + \Delta a$ is

$$-\frac{1}{\Delta a} \int_a^{a+\Delta a} \rho(x, t) dx = \frac{N(a+\Delta a, t) - N(a, t)}{-\Delta a}.$$

In the limit as $\Delta a \rightarrow 0$, the right-hand side is $-\partial N(a, t)/\partial a$. Using the definition of $N(a, t)$, again from the Fundamental Theorem of Calculus,

$$\frac{\partial N(a, t)}{\partial a} = \rho(a, t).$$

Thus the left-handed side of equation (1.8) again equals $-(\partial/\partial t)\rho(a, t)$. By either method (a) or (b), equation (1.10) holds for all values of a , it is more appropriate to replace a by x , in which case

$$\frac{\partial \rho}{\partial t} + \frac{\partial q}{\partial x} = 0. \quad (1.12)$$

This is a hyperbolic partial differential equation. It expresses a relationship between traffic density and traffic flow derived by assuming that the number of cars is conserved. It is valid everywhere (all x) and for all time. It is called the equation of *conservation of cars*.

1.1.5 A Velocity-Density Relationship

In this subsection a observed traffic phenomenon is described to which we all are no doubt familiar. If traffic is light, the driver of each car has the freedom to do as s/he wishes with certain limitations(example speed limits), each driver will occasionally slow down because of presence of the other vehicles. As traffic increases to mediocre level, each driver encounters a slower moving vehicles more often. Although it is not difficult to pass slower-moving vehicles, but still drivers speed is a wee less than the desired speed. However, in heavy traffic conditions changing lanes becomes difficult, and hence the average speed of the traffic is lowered.

On basis of such observations, a basic simplifying assumption is formulated that at any point along the road the velocity of a vehicle depends only on the density of cars,

$$u = u(\rho). \quad (1.13)$$

Lighthill, M.J. and Whitham, G.B. and independently Richards, P.I. in mid-1950s suggested this type of mathematical model of traffic flow.

If there are no cars on the highway, then the car would travel at the maximum speed u_{max} ,

$$u(0) = u_{max}. \quad (1.14)$$

u_{max} is generally referred to as the "mean free speed" corresponding to the velocity of the cars would move as if they were free from interference from other cars. However, as the density increases gradually the presence of the other cars would slow the car down. As the density increases further the velocities of the cars would continue to decline, and thus

$$\frac{\partial u}{\partial \rho} \equiv u'(\rho) \leq 0. \quad (1.15)$$

At a certain density cars stand still. This maximum density, ρ_{max} , generally corresponds to what is called bumper-to-bumper traffic,

$$u(\rho_{max}) = 0. \quad (1.16)$$

Consequently, the general type of curve shown in figure, $u = u(\rho)$, relating the two traffic variables (velocity and density) is sensible.

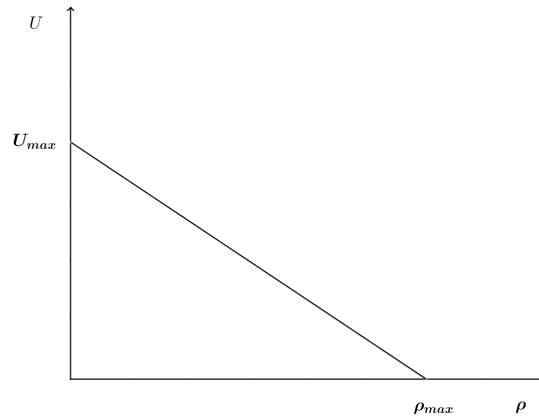


Figure 1.3: Car velocity diminishes as traffic density increases.

1.1.6 Traffic Flow

The traffic flow has certain general properties. The flow may be zero in two significant ways;

1. if there is no traffic ($\rho = 0$), or
2. if the traffic is not moving ($u = 0$ and thus $\rho = \rho_{max}$).

For other values of density ($0 < \rho < \rho_{max}$), the traffic flow must be positive. Thus in general, the traffic flows dependence on density is as illustrated in the figure. This flow-density relationship is generally called the **Fundamental Diagram of Road Traffic**. This shows that a maximum of traffic flow occurs at some density (with a corresponding velocity).

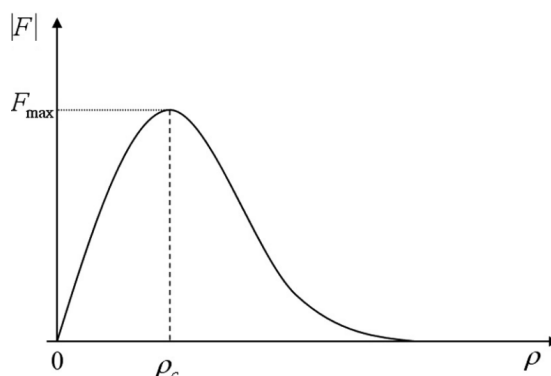


Figure 1.4: Fundamental Diagram of Road Traffic (flow-density traffic).

Where $|F|$ is the flow intensity, F_{max} is the maximum flow which can be attained and ρ_c is the critical density.

1.2 Traffic Assignment Modeling

Traffic assignment models primarily aim to regulate the number of trips on different links of a network with a given travel demand between different pairs of nodes. Such models aspires to mathematically represent the route choice phase of the sequential demand analysis procedure. There are several models of traffic assignment, all of these models assume that travel time on the link is the only factor which trip makers

consider while choosing a route. These models, however, vary in their assumptions regarding the variation in link travel times with the link flow.

Traffic phenomena are nonlinear and complex, depending on the interactions of a large number of vehicles. Due to the individual response of human drivers, vehicles do not interact simply following the laws of mechanics, but rather show phenomena of cluster formation and shock wave propagation, in both forward and backward direction depending on traffic density in a given area. Some mathematical models in traffic flow make use of a vertical queue assumption, where the vehicles along a congested link do not spill back along the length of the link.

Chapter 2

Literature Survey

This chapter covers the critical research carried out in traffic flow including substantive findings, as well as theoretical and methodological contributions to the concerned topic.

2.1 First Order Models

First order traffic flow models have been studied for long time, since they represent the simplest way to begin with the understanding of such a complex system. In this section we provide a brief literature survey of the first order models of traffic flow.

2.1.1 LWR Model [9]

After the names of Lighthill, Whitham and Richards, LWR model considers a unidirectional road on which number of vehicles between any two points are conserved if there are no entrances or exits. The model is given by

$$\frac{\partial q}{\partial x} + \frac{\partial \rho}{\partial t} = 0 \quad (2.1)$$

where

$$q = \rho v \quad (2.2)$$

and q is the flow, ρ is the density and v is the velocity, and the relationship between the traffic density and the mean velocity under steady state is given by

$$v = v_e(\rho) \quad (2.3)$$

Where $v_e(\rho)$ is the equilibrium velocity.

LWR model exhibits a wide range of phenomena such as shock waves and rarefaction waves.

Drawbacks The major drawback of LWR model was that it could not explain magnification of small perturbation in heavy traffic. LWR model also failed to explain different instabilities in traffic flow such as cluster formation. This infact was a issue because all vehicles traveled at equilibrium velocity, v_e .

2.1.2 Greenshield's Experimental Model [12]

Greenshield performed the experiment at the University of Michigan in 1934. His field method of collecting data was quite simple. He used a 16-mm simple movie camera to take pictures on highways. A battery operated camera was used to capture the pictures at regular time intervals. The model is given by:

$$V_e(\rho) = V_{max}\left(1 - \frac{\rho}{\rho_{max}}\right) \quad (2.4)$$

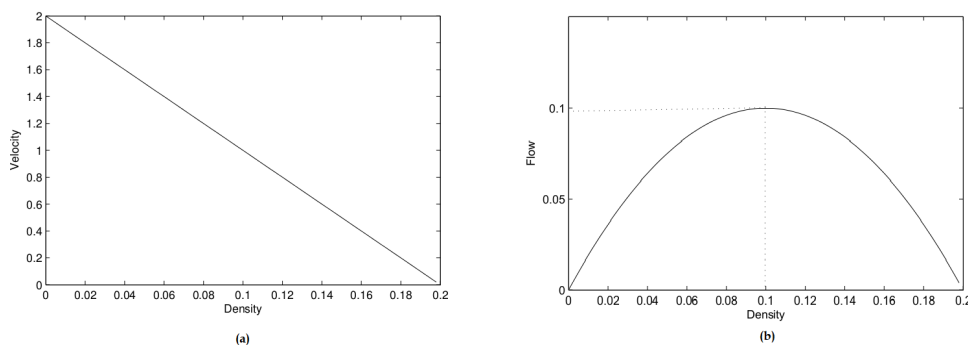


Figure 2.1: (a) A linear velocity-density curve, (b) Fundamental traffic diagram (flow-density curve).

2.2 Higher Order Models

The higher order model of traffic flow, i.e. models with more than one equation (mass, momentum, pressure, etc.) lead to non-physical effects proly because they try to imitate the gas dynamics equation, with a dependence of acceleration.

2.2.1 H.J. Payne's Model [15]

Adding a dynamic equation describing the dynamic of the velocity v . The model is

$$\frac{\partial q}{\partial x} + \frac{\partial \rho}{\partial t} = 0$$

$$\frac{\partial v}{\partial t} + v \frac{\partial v}{\partial x} = \frac{V_e'(\rho) - v}{\tau} + \frac{V_e(\rho)}{2\tau\rho} \frac{\partial \rho}{\partial x} \quad (2.6)$$

where τ is a relaxation time constant, which is the time taken by a driver to adjust its velocity due to front stimuli. This model was the first to explain the formation of cluster effect.

Drawbacks The major drawback of the first order models was that the characteristic speed was greater than the flow velocity, which is also better known as *wrong way travel* problem. This problem defies the general assumption of the traffic flow that flow of a vehicle only travels in one direction and responds to the front stimuli.

2.2.2 Rui Jiang's Model [5]

Jiang *et al.* developed a new continuum traffic flow model based on an improved car-following model. The density gradient in this model was replaced by speed gradient in the equation of motion, which guaranteed that the characteristic speeds will always be less than or equal to the macroscopic flow speed. This model also overcomes backward travel problem which existed in many higher models.

A New Continuum Model This model assumes that the state of the car $n + 1$ at position x represents the average traffic condition at $[x - \frac{1}{2}\Delta, x + \frac{1}{2}\Delta]$, which is determined by the average traffic condition in the preceding region $[x + \frac{1}{2}\Delta, x + \frac{3}{2}\Delta]$. Here Δ corresponds to Δx in car-following theory, and it varies with different inter-vehicle spaces between different successive vehicles. The new improved continuum model consistent with other high-order models, comprises two partial differential equations as follows:

$$\frac{\partial k}{\partial t} + \frac{\partial(ku)}{\partial x} = g(x, t) \quad (2.7)$$

$$\frac{\partial u}{\partial t} + u \frac{\partial u}{\partial x} = \frac{u_e - u}{T} + c_0 \frac{\partial u}{\partial x} \quad (2.8)$$

where u is space mean speed, u_e is equilibrium speed, T is relaxation time, $g(x, t)$ is the generation rate and define

$$c_0 = \frac{\Delta}{\tau},$$

Where τ is the time needed for the backward propagated disturbance to travel a distance of Δ and c_0 represents the propagation speed of the disturbance.

Numerical Scheme Assuming $g(x, t) = 0$ and applying the finite difference method to discretize above equations, we obtain the following difference equations:

$$k_i^{j+1} = k_i^j + \frac{\Delta t}{\Delta x} k_i^j (u_i^j - u_{i+1}^j) + \frac{\Delta t}{\Delta x} u_i^j (k_{i-1}^j - k_i^j) \quad (2.9)$$

(a) if the traffic density is high ($u_i^j < c_0$)

$$u_i^{j+1} = u_i^j + \frac{\Delta t}{\Delta x} (c_0 - u_i^j) (u_{i+1}^j - u_i^j) - \frac{\Delta t}{\Delta T} (u_i^j - u_e) \quad (2.10)$$

(b) if the traffic is light ($u_i^j \geq c_0$)

$$u_i^{j+1} = u_i^j + \frac{\Delta t}{\Delta x} (c_0 - u_i^j) (u_i^j - u_{i-1}^j) - \frac{\Delta t}{\Delta T} (u_i^j - u_e) \quad (2.11)$$

where index i represents the road section and index j represents time. For the discretization of the conservation eq. (2.9), the difference format suitable for physical sense of traffic flow is applied. For the motion equations of (2.10) and (2.11), one-order upwind scheme is applied.

Shock waves and Rarefaction waves In order to evaluate whether the new model can constitute important traffic flow conditions such as shock waves and rarefaction waves, numerical tests are carried out. Traffic flow fronts between a congested and a nearly free traffic evolve under two Riemann initial conditions are investigated further. These two initial conditions are

$$k_u^1 = 0.04(\text{veh}/m), k_d^1 = 0.18(\text{veh}/m), \quad (2.12)$$

$$k_u^2 = 0.18(\text{veh}/m), k_d^2 = 0.04(\text{veh}/m), \quad (2.13)$$

where k_u and k_d are upstream and downstream densities, respectively. Condition (2.12) corresponds to a situation where a nearly free-flow traffic meets a traffic jam, i.e., a shock wave situation. Condition (2.13) corresponds to a situation of a dissolving traffic jam, that is a rarefaction wave situation. Initial speed conditions are

$$u_u^{1,2} = u_e(k_u^{1,2}), \quad u_d^{1,2} = u_e(k_d^{1,2}). \quad (2.14)$$

Free boundary conditions are used here, i.e.,

$$\frac{\partial k}{\partial x} = 0, \quad \frac{\partial u}{\partial x} = 0. \quad (2.15)$$

on both sides. The equilibrium speed-density relationship developed by Del Castillo and Benitez (1995) is applied

$$u_e = u_f \left[1 - \exp \left(1 - \exp \left(\frac{c_m}{u_f} \left(\frac{k_m}{k} - 1 \right) \right) \right) \right] \quad (2.16)$$

where u_f is the free-flow speed; k_m is the maximum density; and c_m is the kinematic wave speed under the jam density. The test road section is $20km$ long, and it is divided into 100 meshes equally, the time interval is $1sec$. Parameter values used are as follows:

$$u_f = 30 \text{ m/sec}; \quad k_m = 0.2 \text{ veh/m}; \quad T = 10 \text{ sec}; \quad c_m = c_0 = 11 \text{ m/sec}.$$

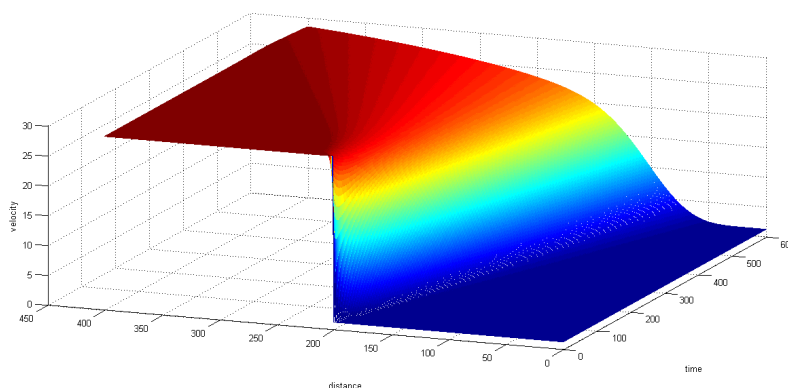


Figure 2.2: Rarefaction wave under the Riemann initial condition: temporal development of speed $u(x, t)$.

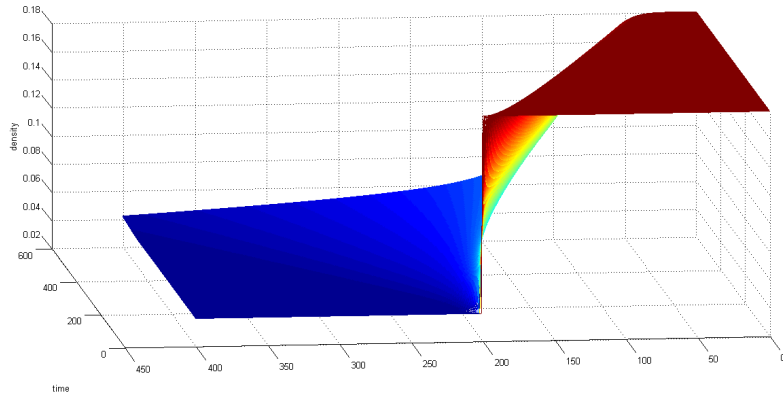


Figure 2.3: Rarefaction waves under the Riemann initial condition: temporal development of density $k(x, t)$

From figure, we see that Jiang's new model provides correct predictions under the two Riemann initial condition. Different Riemann initial conditions lead to different fronts between the congested and the free-flow traffic.

Chapter 3

A Continuum Model for Urban Cities

Jiang et al. proposed a predictive continuum dynamic user-optimal (PDUO-C) model to investigate the dynamic characteristics of traffic flow and the corresponding route-choice behavior of travelers. The modeled region is a dense urban city, which is arbitrary in shape and has a single central business district (CBD).

3.1 Problem Description

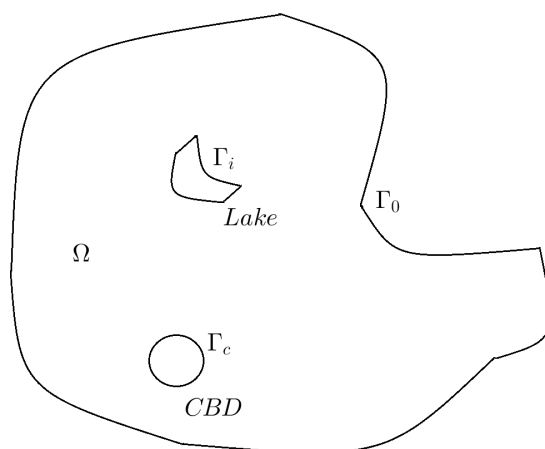


Figure 3.1: The Modeling Domain

The modeled region is an urban city denoted by Ω . Let Γ_0 be the outer boundary of the city, let Γ_c be the boundary of the compact CBD, and let Γ_i be the boundary

of an obstruction such as a lake or an undeveloped area, where traffic is not allowed to enter. Thus, the boundary of Ω is,

$$\Gamma = \Gamma_0 \cup \Gamma_c \cup \Gamma_i.$$

The travelers homes are assumed to be continuously located along $(x, y) \in \Omega$. Everyone travels to the CBD within the modeling region for a given time-dependent demand.

The variables are noted as follows:

- $\rho(x, y, t)$ (in (veh/km^2)) is the density of the travelers at the location (x, y) at time t .

Since it is assumed that no traveler is allowed to leave the city by crossing boundary Γ_0 or to enter the obstruction through Γ_i , we have

$$\rho(x, y, t) = 0, \forall (x, y) \in \Gamma_0 \cup \Gamma_i, t \in T$$

Where $T = [0, t_{end}]$ (in h) is the modeling period.

- $V = (u(x, y, t), v(x, y, t))$ is the velocity vector at location (x, y) at time t .
- $U(x, y, t)$ (in (Km/h)) is the speed, which is the norm of the velocity vector, *i.e.*, $U = |V|$.
- $F = (f_1(x, y, t), f_2(x, y, t))$ is the flow vector at location (x, y) at time t , which is defined as $F = \rho V$.
- $q(x, y, t)$ (in $(veh/km^2/h)$) is the travel demand at location (x, y) at time t .
- $c(x, y, t)$ (in $(Rs./km)$) is the travel cost per unit distance of travel at location (x, y) at time t .
- $\phi(x, y, t)$ is the total travel cost incurred by a traveler who departs from location (x, y) at time t to travel to the CBD.

A path-choice strategy is constructed and a model to this problem is developed in order to investigate the relationship between different variables. Road network is assumed to be very dense and travelers are free to move around it. This model also assumes that travelers have complete information about traffic conditions over time, so that they choose their path such that the actual travel cost (not the instantaneous travel cost) is minimized, thus resulting in a predictive user-equilibrium for a dynamic system.

3.2 Inconsistency of the Jiang's model

3.2.1 Original Model (Jiang et al.) [7]

Jiang et al. (2011) developed a PDUO model to solve this problem. In their path-choice strategy, the following two conditions were required:

$$(u, v, 1) \parallel -(\phi_x, \phi_y, \phi_t) \quad (3.1)$$

and

$$|\bar{\nabla}\phi| = \frac{cU}{\sqrt{U^2 + 1}}, \quad (3.2)$$

Where \parallel denotes that two vectors are parallel and $\bar{\nabla} = (\frac{\partial}{\partial x}, \frac{\partial}{\partial y}, \frac{\partial}{\partial t})$.

It has been proved that under these two conditions, travelers choose their path to the CBD in a dynamic predictive user-optimal manner.

The model proposed by Jiang et al. can be solved by:

$$\begin{cases} \rho_t + \nabla \cdot F = q, & \forall (x, y) \in \Omega, t \in T, \\ F = -\rho U \frac{\nabla \phi}{|\nabla \phi|}, & \forall (x, y) \in \Omega, t \in T, \\ |\nabla \phi| = \frac{cU^2}{U^2 + 1}, & \forall (x, y) \in \Omega, t \in T, \\ \phi_t + \frac{1}{U} |\nabla \phi|, & \forall (x, y) \in \Omega, t \in T, \end{cases} \quad (3.3)$$

subject to the initial boundary conditions

$$\begin{cases} \rho(x, y, 0) = \rho_0(x, y), & \forall (x, y) \in \Omega, \\ \rho(x, y, t) = 0, & \forall (x, y) \in \Gamma_0 \cup \Gamma_i, t \in T, \\ \phi = \phi_{CBD}, & \forall (x, y) \in \Gamma_c, t \in T, \end{cases} \quad (3.4)$$

Where $\nabla = (\frac{\partial}{\partial x}, \frac{\partial}{\partial y})$.

3.2.2 The Inconsistency [2]

Considering a steady state problem, where the cost ϕ is time independent, i.e., $\phi_t = 0$. In this case, eq. (3.1) becomes $(u, v, 1) \parallel (\phi_x, \phi_y, 0)$, which is evidently undesirable, on the other hand the last equation of the model in eq. (3.3) is derived from a deficient path choice strategy. Clearly the units of the terms in this equation are inconsistent

i.e., equation is dimensionally incorrect.

3.3 An Improved Model (Du et al.) [2]

Due to the inconstancy in the original PDUO-C model, an improved model is developed to solve the PDUO-C problem. Hence a path-choice strategy for the case in which the only cost is the travel time is constructed.

3.3.1 The derivation of the path-choice strategy in the special case that the cost is the time

Consider a case in which the cost is the travel time in the domain, as shown in figure (3.2). $x - y$ plane is used to represent the space domain in which the vehicles move. The vertical axis represents the time. Let the coordinate of point A in the $x - y$ plane be (x, y) . The curve that passes point (x, y, t) represents the 3D trajectory of a vehicle passing point A at time t and heading toward the CBD in the time-space domain.

Definition 3.1. *The Departure Time*

We denote $z(x, y, t_D)$ as the departure time at point (x, y) , such that a vehicle can arrive CBD at time t_D along the speed trajectory.

Consider the derivation of the equation to compute $z(x, y, t_D)$. For a time t_D , we see $z(x, y, t_D)$ as a surface in the time-space domain. A vehicle can reach the CBD at time t_D on this surface, when moving along the given speed trajectory. Define a path on this surface as $(x(t), y(t), t)$ with the parameter t , and the position of the CBD is $(x(t_D), y(t_D))$. We have

$$z(x(t), y(t), t_D) = t. \tag{3.5}$$

Hence along this path, we have

$$\frac{dz}{dt} = \frac{\partial z}{\partial x} \frac{dx}{dt} + \frac{\partial z}{\partial y} \frac{dy}{dt} = 1. \tag{3.6}$$

Since $\frac{dx}{dt} = u(x, y, t) = u(x, y, z(x, y, t_D))$ and $\frac{dy}{dt} = v(x, y, t) = v(x, y, z(x, y, t_D))$, we can obtain the following equation to compute $z(x, y, t_D)$:

$$\begin{cases} \frac{\partial z(x, y, t_D)}{\partial x} u(x, y, z(x, y, t_D)) + \frac{\partial z(x, y, t_D)}{\partial y} v(x, y, z(x, y, t_D)) = 1, \\ z(CBD, t_D) = t_D. \end{cases} \tag{3.7}$$

For each t_D , the initial condition is set at time t_D , and this equation can be solved outwards from the CBD, by backtracking in time.

Theorem 1. *If we choose the speed vector V such that the resulting ∇z is always parallel to V and has the same direction, then the dynamic predictive user equilibrium in terms of total travel time to the CBD is satisfied.*

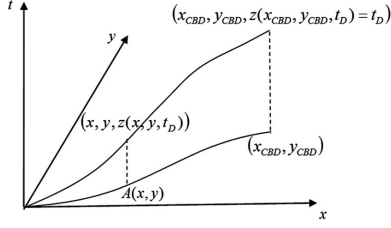


Figure 3.2: The 3D trajectory of a vehicle.

Proof Appendix A.

with the condition $\nabla z \parallel V$, we obtain:

$$\begin{cases} |\nabla z| = \frac{1}{U}, \\ z(CBD, t_D) = t_D. \end{cases} \quad (3.8)$$

3.3.2 Derivation of the path choice formula with a more general cost

So far, the total travel time was used to represent the cost. A more general path-choice strategy for a general local cost function is constructed further. If the speed vector $(u(x, y, t), v(x, y, t))$ in the time-space domain is known, then the cost potential function $\phi(x, y, t)$ can be determined and hence (ϕ_x, ϕ_y) can be determined. (u, v) can be arbitrary, and need not be parallel with (ϕ_x, ϕ_y) . However, the next theorem shows that if we choose the vector (u, v) such that the resulting $-(\phi_x, \phi_y)$ is parallel to (u, v) , then the dynamic user equilibrium is satisfied.

Theorem 2. *If $(u, v) \parallel (-\phi_x, -\phi_y)$, then the predictive dynamic user equilibrium principle is satisfied.*

Proof Appendix B.

$\phi(x, y, t)$ is now computed when the speed vector is known. The vector (u, v) requires to be defined in a way such that the resulting $-(\phi_x, \phi_y)$ is parallel to it. Also a path is defined along this given speed vector as $(x(t), y(t), t)$ with parameter t . Along this path, we have

$$\frac{d\phi}{dt} = \phi_x \frac{dx(t)}{dt} + \phi_y \frac{dy(t)}{dt} + \phi_t \quad (3.9)$$

By the definition of derivative, we have

$$\begin{aligned} \frac{d\phi}{dt} &= \lim_{\Delta t \rightarrow 0} \frac{\phi(x(t + \Delta t), y(t + \Delta t), t + \Delta t) - \phi(x(t), y(t), t)}{\Delta t} \\ &= -U(x(t), y(t), t) \lim_{\Delta t \rightarrow 0} \frac{\phi(x(t), y(t), t) - \phi(x(t + \Delta t), y(t + \Delta t), t + \Delta t)}{\Delta t U(x(t), y(t), t)}. \end{aligned} \quad (3.10)$$

By combining eqs. (3.9) and (3.10), we obtain the equation to solve ϕ :

$$\frac{1}{U} \phi_t - |\nabla \phi| = -c, \quad (3.11)$$

which is Hamilton Jacobi Equation.

3.3.3 Relation between the Special Case and the General Case

In Section 3.3.1, we denoted $z(x, y, t_D)$ as the departure time from point (x, y) such that the vehicle can arrive at the CBD at time t_D . Thus, in the special case in which the cost $\phi(x, y, t)$ is the travel time from point (x, y, t) to the CBD, we have

$$\phi(x, y, z(x, y, t_D)) = t_D - z(x, y, t_D). \quad (3.12)$$

we can then obtain

$$\begin{cases} \phi_x + \phi_t \cdot z_x = -z_x, \\ \phi_y + \phi_t \cdot z_y = -z_y, \end{cases} \quad (3.13)$$

i.e.,

$$\begin{cases} \phi_x = -(\phi_t + 1)z_x, \\ \phi_y = -(\phi_t + 1)z_y \end{cases} \quad (3.14)$$

Theorem 3. *In the case that the cost $\phi(x, y, t)$ is the travel time in the domain, we have $\phi_t \geq -1$.*

Proof Appendix C.

Using Theorem (3) and eq.(3.14), we have

$$-(\phi_x, \phi_y) \parallel (z_x, z_y).$$

Hence, the requirement of $(u, v) \parallel -(\phi_x, \phi_y)$ and $(u, v) \parallel (z_x, z_y)$ are actually the same.

3.4 The complete model and the discussion of initial boundary conditions [2]

So far, a general path-choice strategy has been discussed. In this section, some proper equations and their initial boundary conditions are presented to construct a complete model using this new path-choice strategy.

3.4.1 The conservation law and its initial boundary conditions

Similar to flow conservation in fluid dynamics, the density $\rho(x, y, t)$ is governed by the following flow conservation law:

$$\rho_t + \nabla \cdot F = q, \forall (x, y) \in \Omega, t \in T, \quad (3.15)$$

where $\rho_t = \frac{\partial \rho}{\partial t}$ and $\nabla = (\frac{\partial}{\partial x}, \frac{\partial}{\partial y})$, a vector $\mathbf{v} = (u, v)$ is chosen in a way such that the resulting $-(\phi_x, \phi_y)$ is parallel to (u, v) , then the dynamic user equilibrium is satisfied. Hence, we have

$$F = \rho \mathbf{v} = -\rho U \frac{\nabla \phi}{|\nabla \phi|}, \quad (3.16)$$

With the assumption that no vehicle is allowed to enter the restricted area through the boundary Γ_c or leave the city through Γ , we define the boundary condition

$$\rho(x, y, t) = 0, \forall (x, y) \in \Gamma_0 \cup \Gamma_i, t \in T, \quad (3.17)$$

In the physical sense, the density in the current time results from the density at present and its variation in the past. Hence, the initial time is set as $t = 0$ and the conservation law is solved along the positive time direction. Here, let $\rho_0(x, y)$ be the density of traffic at location (x, y) at the beginning of the modeling period, and set the initial condition as

$$\rho(x, y, 0) = \rho_0(x, y), \forall (x, y) \in \Omega. \quad (3.18)$$

3.4.2 The Hamilton-Jacobi equation and its initial boundary conditions

To solve the aforesaid conservation law, the travel cost ϕ is still required to compute the flow vector. The travel cost is then solved by the Hamilton-Jacobi equation,

$$\frac{1}{U} \phi_t - |\nabla \phi| = -c, \quad (3.19)$$

Let ϕ_{CBD} represents the boundary value of ϕ and can be explicated as the cost incurred to the traveler entering the CBD:

$$\phi(x, y, t) = \phi_{CBD}, \forall (x, y) \in \Gamma_c, t \in T, \quad (3.20)$$

The initial condition to the Hamilton Jacobi still requires to be defined. Note that the travel cost to the CBD only depends on the events that will occur in the future, and has nothing to do with events that happened in the past. Hence, it seems sensible to solve the Hamilton-Jacobi equation along the negative time direction, thus we set the initial time at $t = t_{end}$. Here, all travelers are assumed to be entered the CBD and there is no traffic in the city at $t = t_{end}$. This can be considered as a static state and the travel cost to the CBD is the instantaneous cost. Following Huang et al.[4] (2009), a 2D Eikonal equation is used to solve the initial values $\phi_0(x, y)$:

$$\begin{cases} |\nabla \phi_0(x, y)| = c(x, y, t_{end}), & \forall (x, y) \in \Omega \\ \phi(x, y, t) = \phi_{CBD}, & \forall (x, y) \in \Gamma_c. \end{cases} \quad (3.21)$$

3.4.3 The Complete Model

We can write our model in two parts.

The CL part is:

$$\begin{cases} \rho_t + \nabla \cdot F = q, & \forall (x, y) \in \Omega, t \in T, \\ F = -\rho U \frac{\nabla \phi}{|\nabla \phi|}, & \forall (x, y) \in \Omega, t \in T, \\ \rho(x, y, t) = 0, & \forall (x, y) \in \Gamma_0 \cup \Gamma_i, t \in T, \\ \rho(x, y, 0) = \rho_0(x, y), & \forall (x, y) \in \Omega. \end{cases} \quad (3.22)$$

The HJ part is:

$$\begin{cases} \frac{1}{U} \phi_t - |\nabla \phi| = -c, & \forall (x, y) \in \Gamma, t \in T, \\ \phi(x, y, t) = \phi_{CBD}, & \forall (x, y) \in \Gamma_c, t \in T, \\ \phi(x, y, t_{end}) = \phi_0(x, y), & \forall (x, y) \in \Gamma. \end{cases} \quad (3.23)$$

where the initial value $\phi_0(x, y)$ is computed by a 2D Eikonal equation:

$$\begin{cases} |\nabla \phi_0(x, y)| = c(x, y, t_{end}), & \forall (x, y) \in \Omega, \\ \phi(x, y, t) = \phi_{CBD}, & \forall (x, y) \in \Gamma_c. \end{cases} \quad (3.24)$$

3.5 Solution Algorithm [2]

In this section, solution algorithms used to solve the improved model are discussed, including the Lax-Friedrichs scheme to solve the conservation law equation, the Lax-Friedrichs scheme to solve the Hamilton-Jacobi equation, the fast sweeping method to solve the Eikonal equation, and the self-adaptive MSA to solve the fixed-point problem.

3.5.1 Lax-Friedrichs scheme to solve the conservation law

In this subsection, the cost potential function $\phi(x, y, t)$ is assumed to be known for all $(x, y) \in \Gamma$ and $t \in T$, and hence the numerical method to solve the conservation law is focused:

$$\begin{cases} \rho_t + \nabla \cdot F = q, & \forall (x, y) \in \Omega, t \in T, \\ F = -\rho U \frac{\nabla \phi}{|\nabla \phi|}, & \forall (x, y) \in \Omega, t \in T, \\ \rho(x, y, t) = 0, & \forall (x, y) \in \Gamma_0 \cup \Gamma_i, t \in T, \\ \rho(x, y, 0) = \rho_0(x, y), & \forall (x, y) \in \Omega. \end{cases} \quad (3.25)$$

The conservative difference scheme is used to approximate the point values $\rho_{i,j}^n \approx \rho(x_i, y_j, t^n)$:

$$\rho_{i,j}^{n+1} = \rho_{i,j}^n - \frac{\Delta t}{\Delta x} (\hat{f}_{i+\frac{1}{2},j} - \hat{f}_{i-\frac{1}{2},j}) - \frac{\Delta t}{\Delta y} (\hat{g}_{i,j+\frac{1}{2}} - \hat{g}_{i,j-\frac{1}{2}}), \quad (3.26)$$

where $q_{i,j} = q(x_i, y_j, t^n)$ is defined as the given travel demand at location (x_i, y_j) at time t^n , Δx and Δy are the mesh sizes in x and y directions, respectively, and $\hat{f}_{i+\frac{1}{2},j}$ and $\hat{g}_{i,j+\frac{1}{2}}$ are the numerical fluxes in the x and y directions, respectively and are defined as,

$$\hat{f}_{i+\frac{1}{2},j} = \frac{1}{2} [f(\rho_{i,j}^n) + f(\rho_{i+1,j}^n) - \alpha_f (\rho_{i+1,j}^n - \rho_{i,j}^n)] \quad (3.27)$$

$$\hat{g}_{i,j+\frac{1}{2}} = \frac{1}{2} [f(\rho_{i,j}^n) + f(\rho_{i,j+1}^n) - \alpha_g (\rho_{i,j+1}^n - \rho_{i,j}^n)] \quad (3.28)$$

Where $\alpha_f = \max |f'(\rho)|$ and $\alpha_g = \max |g'(\rho)|$.

3.5.2 Lax-Friedrichs scheme to solve the Hamilton-Jacobi equation

In this subsection, the density $\rho(x, y, t)$ is assumed to be known for all $(x, y) \in \Omega$ and $t \in T$, and hence the numerical method to solve Hamilton-Jacobi equation is focused:

$$\begin{cases} \frac{1}{U} \phi_t - |\nabla \phi| = -c, & \forall (x, y) \in \Gamma, t \in T, \\ \phi(x, y, t) = \phi_{CBD}, & \forall (x, y) \in \Gamma_c, t \in T, \\ \phi(x, y, t_{end}) = \phi_0(x, y), & \forall (x, y) \in \Gamma. \end{cases} \quad (3.29)$$

Note that the initial time is $t = t_{end}$ and the initial value $\phi_0(x, y)$ is computed by the Eikonal equation. In this subsection $\phi_0(x, y)$ is assumed to be known. As the initial time is $t = t_{end}$, define

$$\tau = t_{end} - t, \Phi(x, y, \tau) = \phi(x, y, t_{end} - t), \quad (3.30)$$

thus the time-dependent HJ equation is rewritten into the usual form:

$$\begin{cases} \frac{1}{U}\Phi_\tau - |\nabla\Phi| = c, & \forall(x, y) \in \Gamma, \tau \in T, \\ \Phi(x, y, \tau) = \phi_{CBD}, & \forall(x, y) \in \Gamma_c, \tau \in T, \\ \Phi(x, y, 0) = \phi_0(x, y), & \forall(x, y) \in \Gamma. \end{cases} \quad (3.31)$$

Define

$$H(\Phi_x, \Phi_y) = U(|\nabla\Phi| - c), \quad (3.32)$$

then the scheme to solve $\Phi_\tau + H(\Phi_x, \Phi_y) = 0$ is

$$\Phi_{i,j}^{n+1} = \Phi_{i,j}^n - \Delta t \hat{H}((\Phi_x)_{i,j}^-, (\Phi_x)_{i,j}^+, (\Phi_y)_{i,j}^-, (\Phi_y)_{i,j}^+), \quad (3.33)$$

where

$$(\Phi_x)_{i,j}^- = \frac{\Phi_{i,j} - \Phi_{i-1,j}}{\Delta x}, \quad (\Phi_x)_{i,j}^+ = \frac{\Phi_{i+1,j} - \Phi_{i,j}}{\Delta x} \quad (3.34)$$

$$(\Phi_y)_{i,j}^- = \frac{\Phi_{i,j} - \Phi_{i,j-1}}{\Delta y}, \quad (\Phi_y)_{i,j}^+ = \frac{\Phi_{i,j+1} - \Phi_{i,j}}{\Delta y} \quad (3.35)$$

and \hat{H} is a Lipschitz continuous monotone flux consistent with H . Here, global Lax-Friedrichs flux is used:

$$\hat{H}(u^-, u^+, v^-, v^+) = H\left(\frac{u^- + u^+}{2}, \frac{v^- + v^+}{2}\right) - \frac{1}{2}\alpha^x(u^- + u^+) - \frac{1}{2}\alpha^y(v^- + v^+), \quad (3.36)$$

where α^x and α^y are the viscosity constants and are defined as

$$\alpha^x = \max_{A \leq u \leq B, C \leq v \leq D} |H_1(u, v)|, \quad \alpha^y = \max_{A \leq u \leq B, C \leq v \leq D} |H_2(u, v)| \quad (3.37)$$

$H_1(H_2)$ is the partial derivative of H in terms of $\Phi_x(\Phi_y)$, $[A, B]$ is the value range of u^\pm and $[C, D]$ is the value range of v^\pm .

3.6 Fixed-point problem and MSA

The two parts of the model are completely intertwined. While computing the density ϕ by solving the CL, the total cost ϕ of getting to the CBD from every point must be known, and thus the direction of flow needed to compute the density at the next

time level can be decided. While computing the cost ϕ by solving the HJ, the density information must be known in order to obtain the local cost. However, neither ρ nor ϕ is known initially, also these two parts cannot be solved together as they have different initial times. As a matter of fact this model is in fact a fixed-point problem that can be solved by the Method of Successive Averages (MSA).

Define the vector of the numerical solutions at each grid point and each time level as

$$\vec{\rho} = \{\rho_{i,j}^n, i = 1, \dots, N_x, j = 1, \dots, N_y, n = 1, \dots, N_t\} \quad (3.38)$$

$$\vec{\phi} = \{\phi_{i,j}^n, i = 1, \dots, N_x, j = 1, \dots, N_y, n = 1, \dots, N_t\} \quad (3.39)$$

where N_x , N_y and N_t are the number of grid points in x, y and t, respectively.

Definition of **one iteration**, which contains two steps is discussed further,

Step 1 With a given vector $\vec{\phi}^{old}$ the CL eq. is solved from $t = 0$ to $t = t_{end}$ using Lax-Friedrichs Scheme, thus the vector $\vec{\rho}$ is obtained

$$\vec{\rho} = g(\vec{\phi}^{old}) \quad (3.40)$$

Step 2 The HJ eq. is solved from $t = t_{end}$ to $t = 0$ using the Lax-Friedrichs scheme so as to obtain the updated vector $\vec{\phi}^{new}$. This step is denoted as

$$\vec{\phi}^{new} = h(\vec{\rho}) \quad (3.41)$$

Step 1 and Step 2 are considered as one iteration and is further denoted as

$$\vec{\phi}^{new} = h(g(\vec{\phi}^{old})) = f(\vec{\phi}^{old}) \quad (3.42)$$

With the definition of one iteration and the function f , the model translates to a fixed-point problem

$$\vec{\phi} = f(\vec{\phi}) \quad (3.43)$$

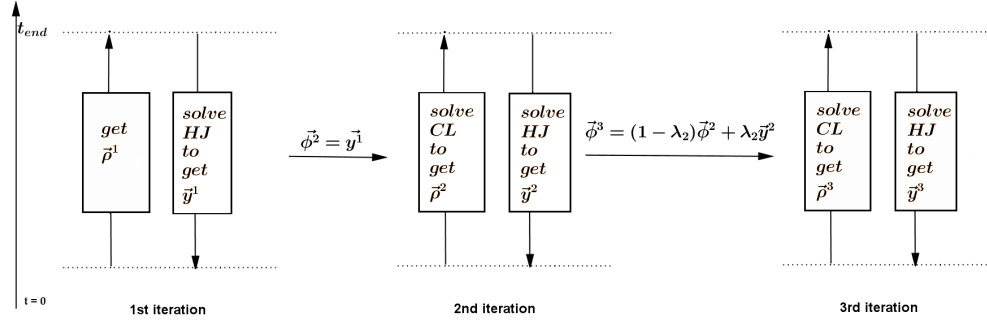


Figure 3.3: Solution Procedure

which can be solved by the MSA.

The MSA was first introduced by Robbins and Monro[10], (1951) to solve the fixed-point problem. A general MSA is an iterative process. Denote the solution before k th iteration as $\vec{\phi}^k$, then computing the MSA to obtain $\vec{\phi}^{k+1}$ involves the following steps:

Step 1. Solve the temporary solution $\vec{y}^k = f(\vec{\phi}^k)$ during the k th iteration.

Step 2. Choose a step size λ_k and use the following equation to obtain $\vec{\phi}^{k+1}$:

$$\vec{\phi}^{k+1} = (1 - \lambda_k)\vec{\phi}^k + \lambda_k \cdot \vec{y}^k, k = 1, 2, \dots \quad (3.44)$$

Convergence is declared if

$$\|\vec{\phi}^{k+1} - \vec{\phi}^k\| \leq \delta. \quad (3.45)$$

where δ is a given convergence threshold value. We use $\delta = 10^{-2}$ and L_2 as the norm in our computation.

3.6.1 A self-adaptive MSA [2]

Assume a smooth function f , which derives the following formula:

$$\frac{\|\vec{\phi}^{k+1} - f(\vec{\phi}^{k+1})\|^2}{\|\vec{\phi}^k - f(\vec{\phi}^k)\|^2} \rightarrow r^*(\lambda) \quad (3.46)$$

where k is the constant step size and $r^*(\lambda)$ is a convex quadratic function that is pointing up. In addition, $r^*(0) = 1$ and $\frac{\partial r^*}{\partial \lambda}(0) < 0$. Any constant step size such that $r^*(\lambda) < 1$ results in convergence.

Based on the formula, least squares method is used to fit the curve $r^*(\lambda)$, and set the minimum point λ^* as the updated step size. The procedure for determining the optimal step size used in the self-adaptive MSA is as follows.

1. Predetermined step sizes have been used for the first several iterations,

$$\lambda_1 = 1.0, \lambda_2 = 0.4, \lambda_3 = 0.3, \lambda_4 = 0.2, \lambda_5 = 0.15, \lambda_6 = 0.1, \lambda_7 = 0.05, \quad (3.47)$$

2. After the k th iteration ($k > 2$), the step size λ_{k-1} is recorded which is used before this iteration and the resulting ratio of the error

$$r_{k-1} = \frac{\|\vec{\phi}^k - f(\vec{\phi}^k)\|^2}{\|\vec{\phi}^{k-1} - f(\vec{\phi}^{k-1})\|^2} \quad (3.48)$$

thus constituting a discrete point (λ_{k-1}, r_{k-1}) to fit the curve $r^*(\lambda)$.

3. For the step size $n + 1$ ($n \geq 7$), least squares method is used to fit the discrete points (λ_k, r_k) , $k = 1, \dots, n$ and hence the fitted quadratic curve $r^*(\lambda)$ is obtained. The new step size λ_{n+1} is defined as the minimum of $r^*(\lambda)$, i.e., $r^*(\lambda_{n+1}) = \min_{\lambda} r^*(\lambda)$.
4. Invalid step size such that $\lambda_{n+1} \leq 0$ or $\lambda_{n+1} \geq 1$ is abandoned, and step size is set as $\lambda_{n+1} = 0.5\lambda_n$.

There are several other points to note about the self-adaptive MSA.

- The quadratic curve $r^*(\lambda)$ must pass through the point $(0, 1)$, i.e.,

$$r^*(0) = 1, \quad (3.49)$$

and as such only two parameters must be determined to fit the curve.

- The least squares method is not used until the eighth step because the accuracy of the discrete points (λ_k, r_k) is low for the first several iterations due to the non-linearity of f .
- The first several step sizes λ_k , $k = 2, \dots, 7$ are distributed on the interval $[0, 0.4]$ to avoid concentrating the step size distribution into too narrow a range, which may lead to a poor least squares estimate.

- The descent speed of λ_k , $k = 1, \dots, 7$ is much faster than the conventional step size $\lambda_k = 1/k$ (Robbins and Monro[10], 1951) and hence avoids too large an amplification of the error.
- $\lambda_{n+1} = 0.5\lambda_n$ is reset when $\lambda_{n+1} \leq 0$ or $\lambda_{n+1} \geq 1$ to avoid trying the same non-optimal step size repeatedly, which would not produce a better estimate of the quadratic curve. A small step size can also guarantee convergence.
- The self-adaptive MSA uses the information from the iterations and adjusts the step size accordingly. The step size may be inaccurate at the beginning, but becomes increasingly accurate as the number of iterations, k , increases.

3.7 Numerical Setting [2]

We consider a rectangular domain that is 35 km long and 25 km wide in the numerical computation which is discretized in spatially as 140 grids in x -direction and 100 grids in y -direction. The center of the compact CBD is located at (10 km, 10 km), and a lake is located at (25 km, 15 km). We assume that there is no traffic at the beginning or the end of the modeling period (i.e., $\rho_0(x, y) = 0, \forall(x, y) \in \Omega$), and that no cost is incurred by entering the CBD ($\phi_{CBD} = 0, \forall(x, y) \in \Gamma_c, t \in T$). We set $t_{end} = 6$, and so the modeling period is $T = [0h, 6h]$. The traffic demand function q is defined as

$$q(x, y, t) = q_{max}[1 - \gamma_1 d(x, y)]g(t), \quad (3.50)$$

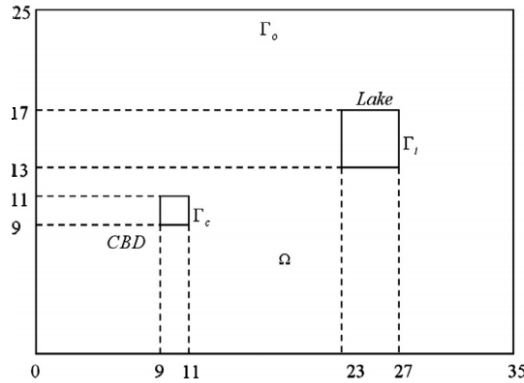


Figure 3.4: The modeling domain.

where $q_{max} = 240 \text{ veh}/\text{km}^2/\text{h}$ is the maximum demand, $\gamma_1 = 0.01 \text{ km}^{-1}$ is a positive scalar and $d(x, y) = \sqrt{(x - 10)^2 + (y - 10)^2}$ is the distance from location

(x, y) to the center of the CBD. The factor $[1 + \gamma_1 d(x, y)]$ is used to express the higher traffic demand generated in the domain closer to the CBD, where more of the population is located. $g(t)$ is a non-negative and time-varying function defined by

$$g(t) = \begin{cases} t, & t \in [0h, 1h] \\ 1, & t \in [1h, 2h] \\ -\frac{4}{5}(t - 3) + \frac{1}{5}, & t \in [2h, 3h] \\ \frac{1}{5}, & t \in [3h, 5h] \\ 0, & t \in [5h, 6h] \end{cases} \quad (3.51)$$

The speed function is defined as $U(x, y) = U_f e^{-\beta \rho^2}$, in which $\beta = 2 \times 10^{-6} \text{ km}^4 \text{ veh}^2$ and $U_f(x, y)$ is the free-flow speed given by

$$U_f(x, y) = U_{max} [1 + \gamma_2 d(x, y)], \quad (3.52)$$

where $U_{max} = 56 \text{ km/h}$ is the maximum speed and $\gamma_2 = 4 \times 10^{-3} \text{ km}^{-1}$. The factor $[1 + \gamma_2 d(x, y)]$ is used to express the faster free-flow speed in the domain far from the CBD, where there are fewer junctions. With this definition, we can compute the critical density of ρ_c as 500 veh/km^2 . The local travel cost per unit of distance is defined as $c(x, y, t) = \kappa \left(\frac{1}{v} + \pi(\rho) \right)$, where $\kappa = 90 \text{ Rs./h}$ and $\pi(\rho) = 10^{-8} \rho^2$. Because we assume that the capacity of the CBD is large enough to accommodate all of the travelers in the city, $|F|$ should maintain the maximum flow intensity F_{max} at the CBD boundary under the congested condition.

We now use the composed algorithm described in the previous section to perform the numerical simulation. A uniform mesh with an $N_x \times N_y$ grid is used. The mesh grids inside the CBD and the mesh grids inside the lake are not computed. The numerical boundary conditions are summarized as follows.

1. On the solid wall boundaries, i.e., the outer boundary of the city, Γ_o , and the boundary of the obstruction, Γ_i , we let the normal numerical flux be 0. We set $\rho = 0$ at the ghost points inside the wall. In the Hamilton-Jacobi equation, the numerical boundary values of ϕ are obtained by extrapolation from inside the computational domain. In the Eikonal equation, we set $\phi = 10^{12}$ at the ghost points.
2. On the boundary of the compact CBD, i.e., Γ_c , we set $\phi = 0$ in both the HJ equation and the Eikonal equation. The boundary conditions for ρ inside the

CBD are obtained by extrapolation from the grids outside the CBD. To maintain the maximum flow intensity $|F| = F_{max}$ on the boundary of the CBD under the congested condition, we set $U(x, y, t) = U_f$ inside the CBD.

3.8 Numerical Results

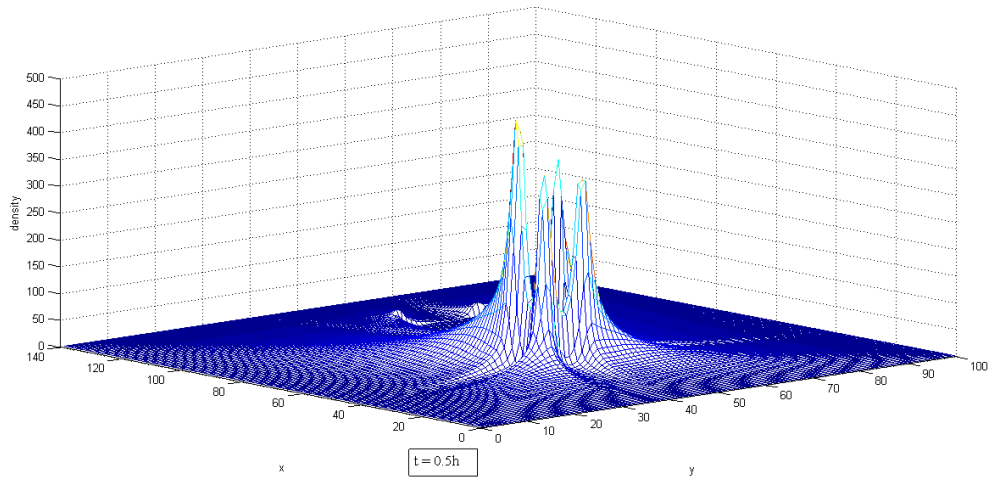


Figure 3.5: Density mesh at $t = 0.5h$

As predicted the density increases near CBD after $0.5 h$ but the magnitude remains low.

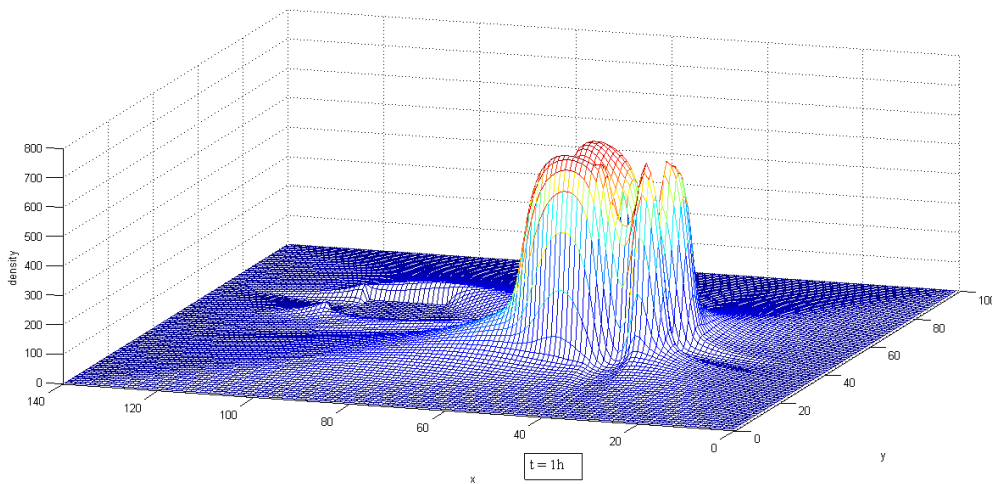


Figure 3.6: Density mesh at $t = 1h$

After $1h$ the density around CBD becomes more prominent and magnitude becomes high.

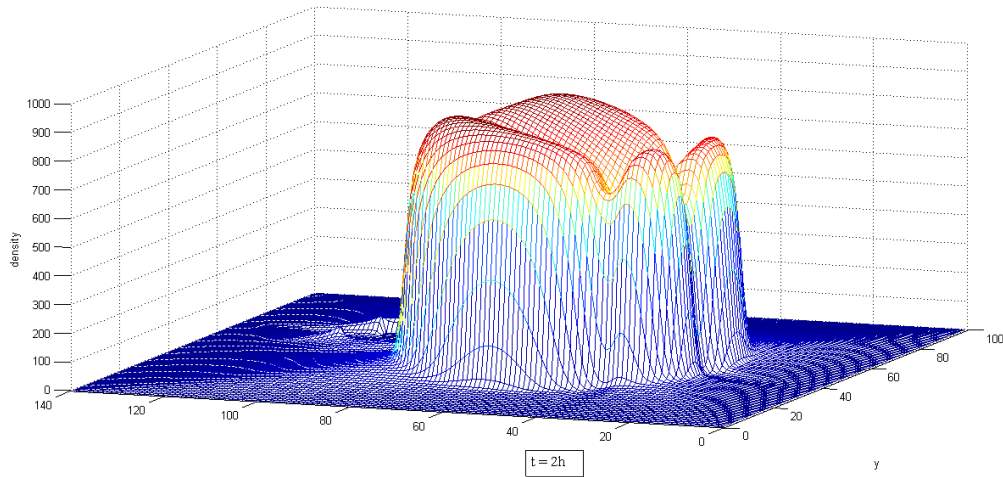


Figure 3.7: Density mesh at $t = 2h$

At $2h$ the density profile around CBD remains same but the magnitude increases.

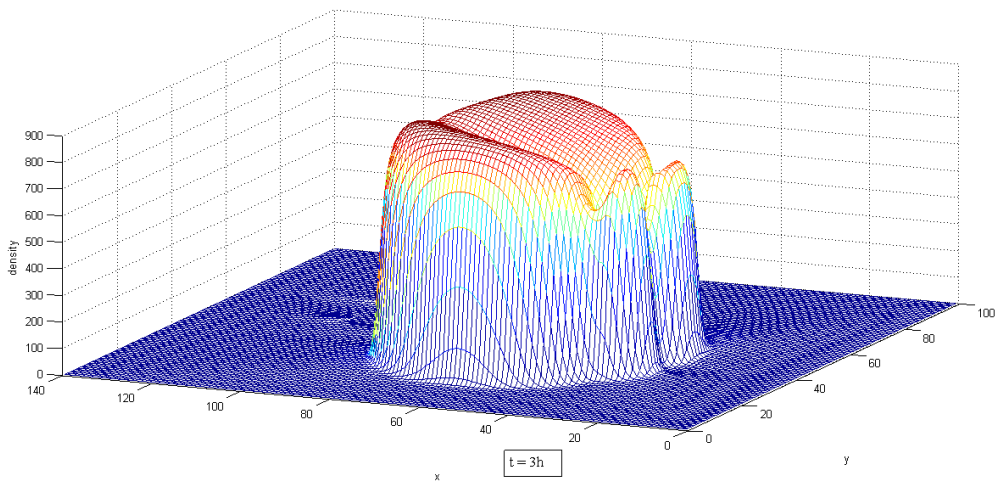


Figure 3.8: Density mesh at $t = 3h$

At $3h$ the density profile around the CBD still remains the same but now the magnitude has started decreasing. This is because a considerable vehicles in the city have now entered the CBD.

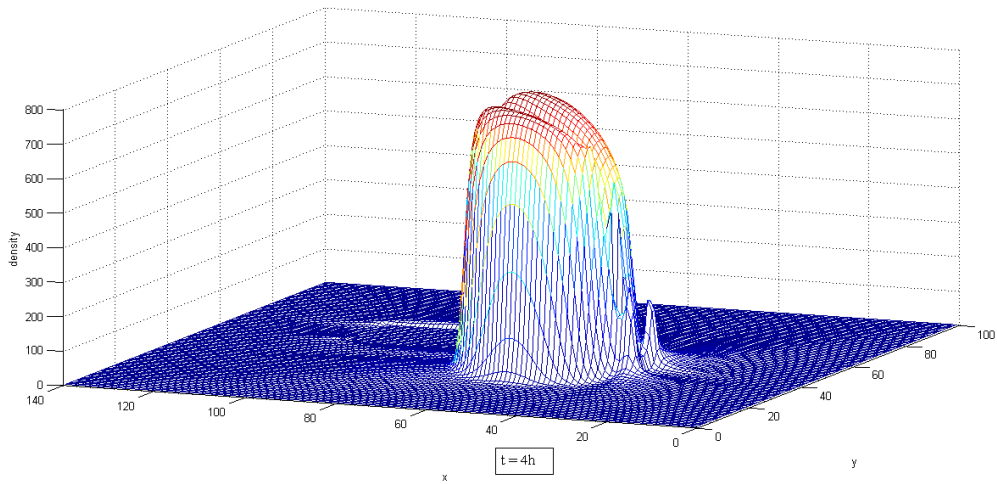


Figure 3.9: Density mesh at $t = 4h$

At $4h$ the density is now scaled down on the side where the city boundaries are near to the CBD but the density is still high on the other side.

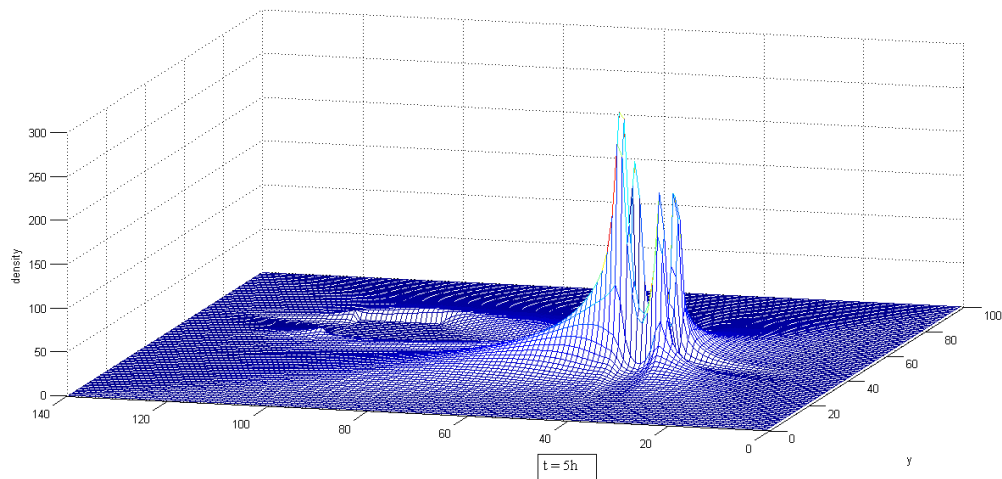


Figure 3.10: Density mesh at $t = 5h$

At $5h$ the density profile resembles as that of $0.5h$. This is because the traffic in the city has now almost saturated.

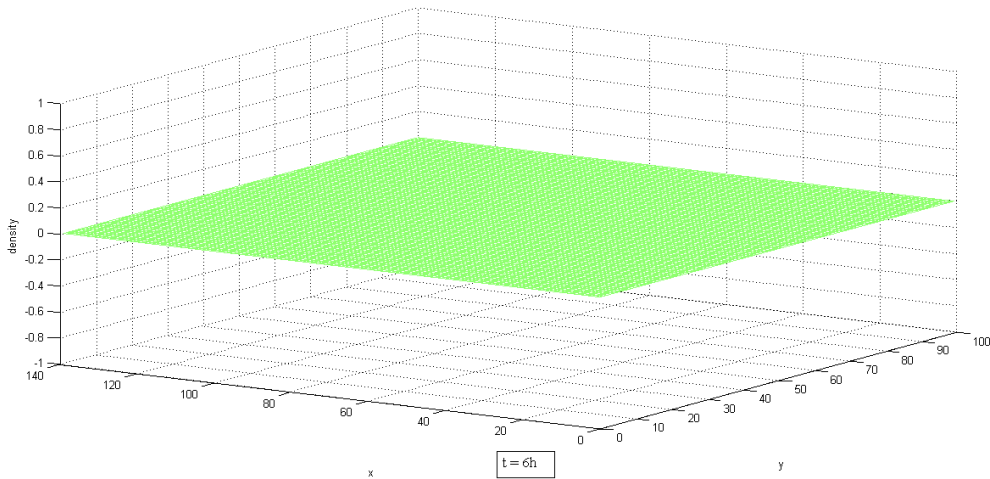


Figure 3.11: Density mesh at $t = 6h$

At $6h$ every one in the city has entered the CBD and hence the density is zero.

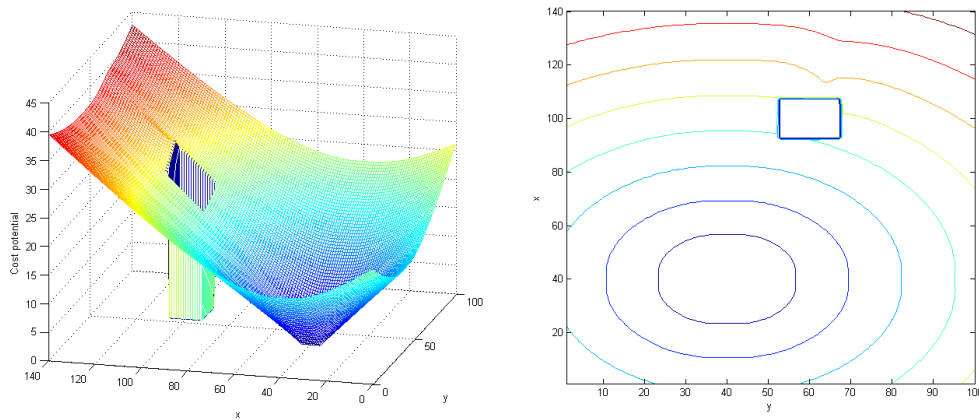


Figure 3.12: Cost potential mesh and contour at $t = 0h$

Initially at $0h$ when the density in the city is zero, the cost potential on the boundaries of CBD is zero and keeps on increasing as we move away from it.

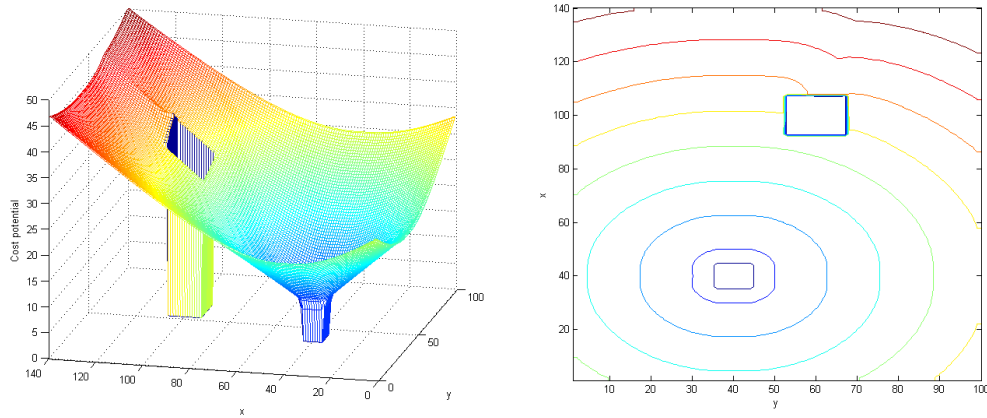


Figure 3.13: Cost potential mesh and contour at $t = 1h$

At $1h$ when the density around the CBD is high the cost incurred to a traveler to move towards the CBD increases.

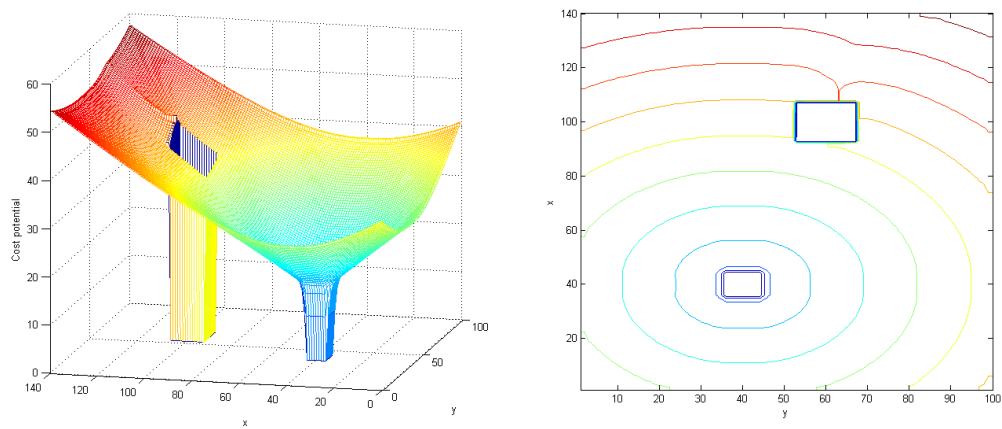


Figure 3.14: Cost potential mesh and contour at $t = 2h$

As the time advances to the end of $2h$ the density becomes even high resulting in the increased cost potential profile.

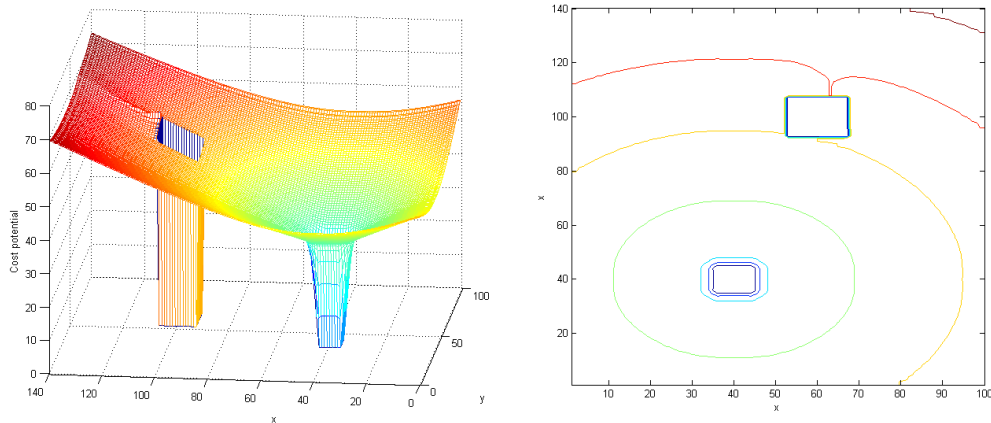


Figure 3.15: Cost potential mesh and contour at $t = 3h$

By the end of $3h$ we observed a diminution in the density profile to which cost potential must also decrease rationally, but our cost potential plots failed to verify this result.

Unfortunately our code was unable to produce the logical results of cost potential profile due to some complexities, since the reason for this uncertainty is still unknown hence a further effort is required to check the computational code and the mathematical model through analysis. The density profiles, however were able to explain few characteristics and was able to capture the complex phenomenon of traffic behavior.

3.9 Conclusions

This project deals with the development and analysis of a mathematical model for traffic assignment problem. A hypothetical test city with one lake and one CBD is modeled and the resulting system of complex partial differential equations is solved numerically. It is shown that the proposed model is able to capture complex phenomena of traffic flow in an urban city. Though the proposed model is able to explain some important characteristics and the results discussed are complete, yet the proposed model will be extended in future to incorporate many important factors like multiple user classes and multiple CDB urban city.

Appendix A

The detailed proof of Theorem 1 [2]

Theorem If we choose the speed vector \mathbf{v} such that the resulting ∇z is always parallel to \mathbf{v} and has the same direction, then the dynamic predictive user equilibrium in terms of total travel time to the CBD is satisfied.

Proof If $\nabla z \parallel \mathbf{v}$, then we have

$$\nabla z \cdot \mathbf{v} = |\nabla z| |\mathbf{v}| = |\nabla z| U, \quad (\text{A.1})$$

where $U = \sqrt{u^2 + v^2}$ is the given isotropic speed in the time-space domain. Using eq. (3.7), we can obtain

$$|\nabla z| U = 1, \quad (\text{A.2})$$

and hence

$$|\nabla z(x, y, t_D)| = 1/U(x, y, z(x, y, t_D)). \quad (\text{A.3})$$

Next, consider fig. (A.1), in which the larger circle has a radius $\Delta t U$, which is the boundary of distance movement in Δt time, as the isotropic speed is U . Here, we assume that Δt is small enough such that $z(x, y, t_D)$ can be treated as a linear function of x and y in such a small area. The dotted curve represents the used path from (x, y) to the CBD based on the parallel condition $\nabla z \parallel \mathbf{v}$. The total travel time along this used path becomes the difference between the departure time $z(x, y, t_D)$ from $(x, y, z(x, y, t_D))$ and the arrival time t_D at the CBD, and thus

$$\phi(x, y, z(x, y, t_D)) = t_D - z(x, y, t_D). \quad (\text{A.4})$$

We need to show that for any path from $(x, y, z(x, y, t_D))$ that deviates from this used path (3D trajectory), the arrival time will be no earlier than t_D , i.e., the total travel time will be no less than $\phi(x, y, z(x, y, t_D))$. We can prove this using the following two steps.

Step 1 Let us first consider an unused path that deviates from the used path only in the first Δt time and then reverts back to the used path. As shown in fig. (A.1), we consider the path that moves away from the starting point with a vector $\Delta t \tilde{\mathbf{v}} = \Delta t(\tilde{u}, \tilde{v})$, where $|\tilde{\mathbf{v}}| = U$ is the isotropic speed, followed by the dashed curve that represents the 3D used trajectory from (\tilde{x}, \tilde{y}) to the CBD, where (\tilde{x}, \tilde{y}) is the position at which the vehicle arrives at the dotted circle boundary in Δt time with the vector $\Delta t \tilde{\mathbf{v}}$. As $\tilde{\mathbf{v}} = (\tilde{u}, \tilde{v})$ is not parallel with $\nabla z = (z_x, z_y)$, by defining the angle between \mathbf{v} and $\tilde{\mathbf{v}}$ as θ , we can show that the change in z at point $(x, y, z(x, y, t_D))$ along the movement vector $\Delta t \tilde{\mathbf{v}}$ is

$$z(\tilde{x}, \tilde{y}) - z(x, y, t_D) = \nabla z \Delta t \tilde{\mathbf{v}} = |\nabla z| |\tilde{\mathbf{v}}| \cos \theta \Delta t = |\nabla z| U \cos \theta \Delta t \leq |\nabla z| U \Delta t \quad (\text{A.5})$$

Here, the first equal sign comes from the assumption that $z(x, y, t_D)$ is a linear function of x and y in this small area. Even without this assumption, as Δt is small enough, the non-linear item in the Taylor expansion is the high order infinitesimal, which makes no difference to our discussion and can be neglected. Using eq. (A.3), we have

$$z(\tilde{x}, \tilde{y}) - z(x, y, t_D) \leq \frac{\Delta t}{U} U = \Delta t, \quad (\text{A.6})$$

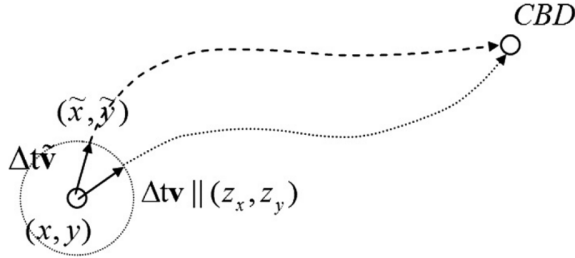


Figure A.1: The used and unused paths.

i.e.

$$z(x, y, t_D) + \Delta t \geq z(\tilde{x}, \tilde{y}). \quad (\text{A.7})$$

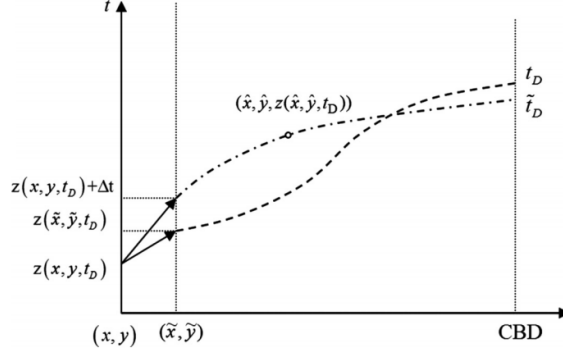


Figure A.2: Two used paths from (\tilde{x}, \tilde{y}) to the CBD.

This means that the arrival time at (\tilde{x}, \tilde{y}) along this unused path, i.e., $z(x, y, t_D) + \Delta t$, will not be earlier than the departure time from (\tilde{x}, \tilde{y}) that is required to reach the CBD at time t_D , i.e., $z(\tilde{x}, \tilde{y})$. The central question is whether a vehicle that departs from (\tilde{x}, \tilde{y}) at a later time could arrive at the CBD earlier than t_D , even if the vehicle follows the used path for the remainder of the journey. We can show that this is not possible by contradiction.

To illustrate this, consider fig. (A.2). Suppose that it is possible to arrive at the CBD at an earlier time \tilde{t}_D , as shown by the dotted-dashed line, even if the vehicle departs later. As $z(x, y, t_D)$ is a closed surface emanating from (CBD, t_D) , the dotted-dashed curve that leaves (\tilde{x}, \tilde{y}) at time $z(x, y, t_D) + \Delta t \geq z(\tilde{x}, \tilde{y})$ and arrives at the CBD at $\tilde{t}_D < t_D$ must cut through the closed surface $z(x, y, t_D)$ somewhere at $(\hat{x}, \hat{y}, z(x, y, t_D))$. However, by definition, if a vehicle departs from this time-space point, it can reach the CBD at both t_D and \tilde{t}_D , which is impossible.

Therefore, if the vehicle moves in any direction other than $\mathbf{v} = (u, v)$ in the first Δt time, it will not arrive at the CBD earlier than t_D , resulting in a total travel time of no less than $\phi(x, y, z(x, y, t_D))$ along the used path.

Step 2 Now let us consider the more general case. In step 1, if a vehicle moves along $\tilde{\mathbf{v}} = (\tilde{u}, \tilde{v})$ in the first Δt time, it will arrive at the CBD at time $\tilde{t}_D \geq t_D$. However, if it does not revert back to the used path in the next step and continues to move in a direction other than the speed vector, then by the same token it will arrive even later at $\tilde{\tilde{t}}_D \geq \tilde{t}_D \geq t_D$. Therefore, for any unused path, the total travel time must be no less than that of the used path.

Appendix B

The detailed proof of Theorem 2 [2]

Theorem If $(u, v) \parallel (-\phi_x, -\phi_y)$, then the predictive dynamic user equilibrium principle is satisfied.

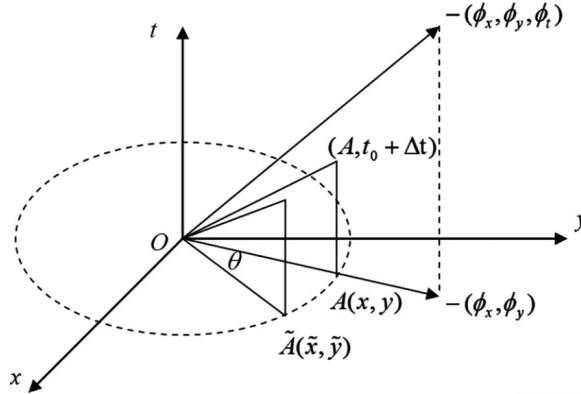


Figure B.1: The used and the unused path.

Proof Recall from the definition in the problem description section that $\phi(x, y, t)$ is the total travel cost incurred by a traveler who departs from location (x, y) at time t to travel to the CBD using the constructed path-choice strategy. This requires traveling along the path that satisfies $(u, v) \parallel (-\phi_x, -\phi_y)$, i.e., the used path. We need to show that for any unused path from $O(x_0, y_0, t_0)$ that deviates from the used path, the total cost must be no less than $\phi(x_0, y_0, t_0)$. We can prove this using the following two steps.

Step 1 We first consider the unused path that deviates from the used path only at the initial Δt time and reverts back to the used path thereafter. Again, we assume

that Δt is small enough such that we can neglect the high order infinitesimal in the Taylor expansion. Consider fig. (B.1), in which the circle has a radius $\Delta t U$, i.e., the boundary of moving Δt time from location $O(x_0, y_0, t_0)$. $A(x, y)$ is the position at which the vehicle arrives along the used path with a vector $\Delta t(u, v)$ based on the parallel condition $(u, v) \parallel (-\phi_x, -\phi_y)$, where $U = \sqrt{u^2 + v^2}$ is the given isotropic speed in the time-space domain. $\tilde{A}(\tilde{x}, \tilde{y})$ is the position at which the vehicle arrives along the unused path with a vector $\Delta t(\tilde{u}, \tilde{v})$. The arrival times at A and \tilde{A} are obviously both $t_0 + \Delta t$. We can show that the change in ϕ along the used path is

$$\begin{aligned}\phi(x, y, t_0 + \Delta t) - \phi(x_0, y_0, t_0) &= (\phi_x, \phi_y, \phi_t) \cdot (u, v, 1) \Delta t \\ &= \Delta t [(\phi_x, \phi_y) \cdot (u, v) + \phi_t] \\ &= \Delta t (-|\nabla \phi| U + \phi_t).\end{aligned}\tag{B.1}$$

The change in ϕ along the unused path is

$$\begin{aligned}\phi(\tilde{x}, \tilde{y}, t_0 + \Delta t) - \phi(x_0, y_0, t_0) &= (\phi_x, \phi_y, \phi_t) \cdot (\tilde{u}, \tilde{v}, 1) \Delta t \\ &= \Delta t [(\phi_x, \phi_y) \cdot (\tilde{u}, \tilde{v}) + \phi_t] \\ &= \Delta t (-|\nabla \phi| U \cos \theta + \phi_t) \\ &\geq \Delta t (-|\nabla \phi| U + \phi_t).\end{aligned}\tag{B.2}$$

Hence, we have

$$\phi(\tilde{x}, \tilde{y}, t_0 + \Delta t) - \phi(x_0, y_0, t_0) \geq \phi(x, y, t_0 + \Delta t) - \phi(x_0, y_0, t_0),\tag{B.3}$$

$$\phi(\tilde{x}, \tilde{y}, t_0 + \Delta t) \geq \phi(x, y, t_0 + \Delta t).\tag{B.4}$$

Note that the travel costs from point $O(x_0, y_0, t_0)$ to A and \tilde{A} are both $\Delta t U c(x, y, t)$. We clearly have

$$\phi(x_0, y_0, t_0) = \Delta t U c(x, y, t) + \phi(x, y, t_0 + \Delta t).\tag{B.5}$$

and the cost along the unused path that deviates from the used path only in the first Δt period is

$$\tilde{\phi} = \Delta t U c(x, y, t) + \phi(\tilde{x}, \tilde{y}, t_0 + \Delta t).\tag{B.6}$$

As $\phi(\tilde{x}, \tilde{y}, t_0 + \Delta t) \geq \phi(x, y, t_0 + \Delta t)$, the total cost along the unused path must be no less than $\phi(x_0, y_0, t_0)$.

Step 2 In the aforementioned case, if a vehicle moves along (\tilde{u}, \tilde{v}) in the first Δt period, it will arrive at the CBD with the cost $\tilde{\phi} \geq \phi(x, y, t_0 + \Delta t)$. However, if it does not revert back to the used path in the next step and continues to move in a direction other than that of the speed vector, then by the same token it will arrive at the CBD with a cost $\tilde{\tilde{\phi}} \geq \tilde{\phi} \geq \phi(x, y, t_0 + \Delta t)$. Therefore, for any unused path, the total cost must be no less than that of the used path.

Appendix C

The detailed proof of Theorem 3 [2]

Theorem In the case that the cost $\phi(x, y, t)$ is the travel time in the domain, we have $\phi_t \geq -1$.

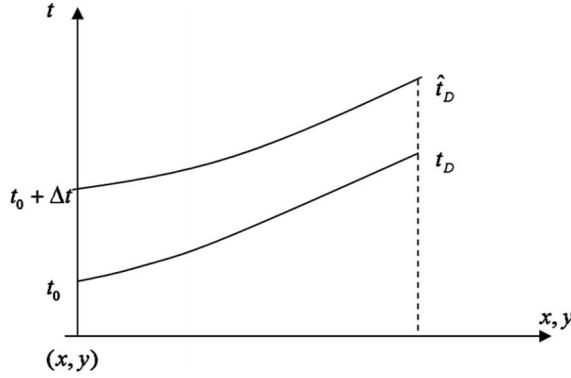


Figure C.1: Two used paths.

Proof The proof is similar to the proof of the dynamic user equilibrium principle in Theorem (1). As shown in fig. (C.1), suppose a vehicle can arrive at the CBD at time t_D along the used path from point (x, y, t_0) , and can arrive at the CBD at time \hat{t}_D along the used path from $(x, y, t_0 + \Delta t)$. From Section (3.3.1), we know that if a vehicle departs from (x, y) at a later time, it will arrive at the CBD later, so we have

$$\begin{cases} \hat{t}_D \geq t_D, & \text{if } \Delta t \geq 0, \\ \hat{t}_D < t_D, & \text{if } \Delta t < 0. \end{cases} \quad (\text{C.1})$$

Now we can estimate the value of ϕ_t as follows:

$$\begin{aligned}
\phi_t &= \lim_{\Delta t \rightarrow 0} \frac{\phi(x, y, t_0 + \Delta t) - \phi(x, y, t_0)}{\Delta t} \\
&= \lim_{\Delta t \rightarrow 0} \frac{[\hat{t}_D - (t_0 + \Delta t)] - [t_D - t_0]}{\Delta t} \\
&= \lim_{\Delta t \rightarrow 0} \frac{\hat{t}_D - t_D}{\Delta t} - 1.
\end{aligned} \tag{C.2}$$

Using eq. (C.1), we get $\phi_t \geq -1$.

Appendix D

Fast sweeping method to solve the Eikonal equation [2]

Before solving the HJ equation, we need the initial value for $\phi_0(x, y)$ to start the numerical computation, which is computed using an Eikonal equation:

$$\begin{cases} |\nabla\phi_0(x, y)| = c(x, y, t_{end}), & \forall(x, y) \in \Omega, \\ \phi_0(x, y) = \phi_{CBD}, & \forall(x, y) \in \Gamma_c, \end{cases} \quad (\text{D.1})$$

where $c(x, y, t) = 90(\frac{1}{U} + 10^{-8}\rho^2)$ and $U(x, y, t) = U_f e^{-\beta\rho^2}$.

The Eikonal equation is in fact a special steady-state Hamilton-Jacobi equation. We use the first-order Godunov fast sweeping method (Zhao[13], 2005) to solve it. We first assign the exact boundary values $\phi_0(x, y) = \phi_{CBD}$ to Γ_c . Large values are assigned as the initial guess values at all other grid points. The following Gauss-Seidel iterations with four alternating direction sweepings are performed:

$$\begin{aligned} (1) \quad & i = 1 : N_x, j = 1 : N_y; & (2) \quad & i = N_x : 1, j = 1 : N_y; \\ (3) \quad & i = N_x : 1, j = N_y : 1; & (4) \quad & i = 1 : N_x, j = N_y : 1, \end{aligned}$$

where i and j are the grid indexes in x and y , respectively. N_x and N_y are the number of grid points in x and y , respectively. When we loop to the point (i, j) , the following formula is used to update the solution:

$$\phi_{i,j}^{new} = \begin{cases} \min(\phi_{i,j}^{xmin}, \phi_{i,j}^{ymain}) + c_{i,j}h, & \text{if } |\phi_{i,j}^{xmin} - \phi_{i,j}^{ymain}| \geq c_{i,j}h, \\ \frac{\phi_{i,j}^{xmin} + \phi_{i,j}^{ymain} + (2c_{i,j}^2 - (\phi_{i,j}^{xmin} - \phi_{i,j}^{ymain})^2)^{\frac{1}{2}}}{2}, & \text{otherwise,} \end{cases} \quad (\text{D.2})$$

where $c_{i,j} = c(x_i, y_j, t_{end})$, $\phi_{i,j}^{x_{min}}$ and $\phi_{i,j}^{y_{min}}$ are defined as

$$\begin{cases} \phi_{i,j}^{x_{min}} = \min(\phi_{i-1,j}, \phi_{i+1,j}), \\ \phi_{i,j}^{y_{min}} = \min(\phi_{i,j-1}, \phi_{i,j+1}). \end{cases} \quad (\text{D.3})$$

Convergence is declared if

$$\|\phi^{new} - \phi^{old}\| \leq \delta, \quad (\text{D.4})$$

where δ is a given convergence threshold value. We use $\delta = 10^{-9}$ and L_1 as the norm in our computation.

Bibliography

- [1] Bar-Gera, H., Boyce, D., Solving a non-convex combined travel forecasting model by the method of successive averages with constant step sizes, *Transportation Research Part B* 40 (5) (2006), 351-367.
- [2] Du, J., Wong, S.C., Shu, Chi-Wang, Xiong, T., Zhang, M., Choi, K., Revisiting Jiangs dynamic continuum model for urban cities 2013, *Transportation Research Part B* 56 (2013) pp 96-119.
- [3] Haberman, 3. *Traffic Flow, Mathematical Models Mechanical Vibrations Population Dynamics and Traffic Flow*, (1998).
- [4] Huang, L., Wong, S.C., Zhang, M.P., Shu, C.W., Lam, W.H.K., Revisiting Hughes dynamic continuum model for pedestrian flow and the development of an efficient solution algorithm, *Transportation Research Part B* 43 (1) (2009), pp 127-141.
- [5] Jiang R., Wu Q.S., Zhu Z.J., A new continuum model for traffic flow and numerical tests, *Transportation Research Part B* 36 (2002), pp 405-419.
- [6] Jiang, Y.Q., Numerical simulation of pedestrian flow past a circular obstruction, *Acta Mechanica Sinica*, 03/16/2011.
- [7] Jiang, Y.Q., Wong, S.C., Ho, H.W., Zhang, P., Liu, R.X., Sumalee, A., A dynamic traffic assignment model for a continuum transportation system. *Transportation Research Part B* 45 (2) (2011), pp 343-363.
- [8] Liu, H.X., He, X.Z., He, B.S., Method of successive weighted averages (MSWA) and self-regulated averaging schemes for solving stochastic user equilibrium problem, *Networks and Spatial Economics* 9 (4) (2009), pp 485-503.

- [9] Lighthill, M.J., Whitham, G.B, On Kinematic Waves. II. A Theory of Traffic Flow on Long Crowded Roads, Proceedings of the Royal Society of London. Series A, Mathematical and Physical Sciences, Vol. 229, No. 1178 (1955), pp. 317-345.
- [10] Robbins, H., Monro, S., A stochastic approximation method, Annals of Mathematical Statistics 22 (3) (1951), pp 400-407.
- [11] Tao, Y. Z., Jiang, Y. Q., Du, J., Wong, S. C., Zhang, P., Xia, Y. H., Choi, K., Dynamic system-optimal traffic assignment for a city using the continuum modeling approach : Continuum DSO Model For The City Transportation, Journal of Advanced Transportation (2013).
- [12] Transportation Research Board, 75 Years of the Fundamental Diagram for Traffic Flow Theory Greenshields Symposium, Transportation Research Circular E-C149 (2011).
- [13] Zhao, H.K., A fast sweeping method for Eikonal equations, Mathematics of Computation 74 (250) (2005), pp 603-627.
- [14] Zhang, H.M., Analyses of the stability and wave properties of a new continuum traffic theory. Transportation Research B 33 (1999), pp 399-415.
- [15] Zhang, H.M., A theory of non-equilibrium traffic flow. Transportation Research B 32 (1998), pp 485-498.